ANALYSIS OF NEGATIVE-SEQUENCE DIRECTIONAL ELEMENT FOR TYPE-IV WIND POWER PLANTS UNDER VARIOUS CONTROL METHODOLOGIES

by

Sathish Kumar Mutha

A thesis submitted to the faculty of
The University of North Carolina at Charlotte
in partial fulfillment of the requirements
for the degree of Master of Science in
Electrical Engineering

Charlotte

2020

Approved by:

_____
Dr. Valentina Cecchi

_____
Dr. Madhav Manjrekar

_____
Dr. Sukumar Kamalasadan

_____
Dr. Arun Shrestha

ABSTRACT

SATHISH KUMAR MUTHA. Analysis of Negative-Sequence Directional Element for Type-IV Wind Power Plants under Various Control Methodologies. (Under the direction of DR. VALENTINA CECCHI)

Negative-sequence directional element operation depends on the magnitude and the phase angle of the negative-sequence current with respect to negative-sequence voltage. The directional element's operation and simplicity of settings lies in the representation of sources with the passive elements in the negative-sequence network diagram. This is not always true for inverter-based resources (IBR) with control schemes that vary from manufacturer to manufacturer. IBR offers specific fault current signature based on the control system and fault ride-through (FRT) conditions defined in the control scheme. This thesis expounds negative-sequence currents for traditional sources and how the negative-sequence directional element uses this behavior to decide the fault direction. Then, a Type IV wind power plant (WPP) with three different control schemes, and an equivalent conventional source model developed in EMTP-RV, are used to generate various faults data. These fault data are used to analyze the behavior of the negative-sequence directional element, developed using the MATLAB tool. This thesis also shows the similarities of the negative-sequence current of the German grid code-based control scheme with traditional sources during unbalanced faults. Recommendations are then made in terms of additional requirements from the German grid code FRT and/or from the negative-sequence directional element logic to achieve improved dependability and security of the directional element.

DEDICATION

This thesis is dedicated to my wife, Dijina A V. without whose bold support and endless love, I would never have been able to complete my graduate studies.

This thesis is also dedicated to my mother, Laxmi Mutha. who is there with me always in my dreams and for my dreams.

ACKNOWLEDGEMENTS

I would first like to thank my faculty advisor, Dr. Valentina Cecchi, at Department of Electrical & Computer Engineering, UNC Charlotte. She helped me a lot academically and non-academically from my very first day at this university. The door to Dr. Cecchi's office was always open whenever I felt out of track or had questions related to a particular course or research topic. She consistently allowed this research to be my own work, but guided me in the right direction whenever she thought I needed it.

I would also like to thank my advisory committee members who were present at every step of this research: Dr. Madhav Manjrekar and Dr. Sukumar Kamalasadan. Taking the courses taught by them aided the advancement of my research work. Without their responsive input, the implementation process would not have been successfully conducted.

I would also like to acknowledge the matchless support from Dr.Arun Shrestha of Schweitzer Engineering Laboratories Inc. He provided me a crucial technical environment to use for my research.

I must express my profound gratitude to my friends and peers: Arunodai Chanda, Rakesh Belchandan, Rasik Sarup, Prashant Morgansgate, Andrew Amuna, Sagar Kanade, Kiran Ravikumar, Abhilash Erukulla, and Bhasker Gaddam for providing me with unfailing support and continuous encouragement throughout my years of study and through the process of researching and writing this thesis. This accomplishment would not have been possible without them. Thank you.

To my children, Chetana Sathish and Sid Vihaan Sathish, thank you for being supportive to your mother, who managed my role also when I was not present during this work, I love you, family.

TABLE OF CONTENTS

LIST OF TABLES ix

LIST OF FIGURES x

LIST OF ABBREVIATIONS xii

CHAPTER 1: INTRODUCTION 1

1.1. Overview 1

1.2. Motivation 1

1.3. Literature Review 3

1.4. Problem Statement 8

1.5. Thesis Overview and Research Contribution 9

1.6. Thesis Organization 10

CHAPTER 2: DIRECTIONAL ELEMENTS, WIND TURBINE GENERATORS AND THEIR CONTROLS 12

2.1. Overview 12

2.2. Various Directional Elements in Protection System 12

2.3. Types of Wind Turbine Generators 20

2.4. Grid Side Controller Modelling Background 25

2.4.1. Phase Locked Loop (PLL) 26

2.4.2. Three-phase Current Control Strategy 30

2.4.3. Grid Filter Modelling 33

2.5. Grid Codes 35

2.5.1. Standards for Distribution Resources 36

2.5.2. Standards for BES Connected Resources 39

2.5.3. VDE-AR-N 4120 (German Grid Code) 42

CHAPTER 3: ANALYSIS OF DIRECTIONAL ELEMENT APPLICATION FOR TRADITIONAL SOURCES AND TYPE-IV WIND POWER PLANTS 44

3.1. Overview 44

3.2. Traditional Sources Short Circuit Behavior 44

3.2.1. Application of Negative-Sequence Directional Element 47

3.3. Type-IV WTG Short Circuit Behavior 49

3.4. Traditional Sources vs German Grid Code-Based Type-IV WPP Negative-Sequence Components Behavior during Faults 51

3.5. Proposed Modification 52

CHAPTER 4: TEST SYSTEM, RESULTS, ANALYSIS AND RECOMMENDATIONS 54

4.1. Overview 54

4.2. Test System 54

4.2.1. WPP Model with Coupled Control (CC) 55

4.2.2. WPP Model with Decoupled Sequence Control-1 58

4.2.3. WPP Model with Decoupled Sequence Control-2 60

4.2.4. Conventional Source Model 61

4.3. Negative-Sequence Directional Element (Software) Settings 61

4.4. Test Results for WPP with CC, DSC-1 and DSC-2 Controls 62

4.5. Test Results for the Conventional Source and WPP with DSC-2 Control 67

4.6. Analysis of Fault Results 71

4.7. Directional Element Results after Implementing the Proposed Modification for Relay Logic 75

4.8. Recommendations 77

CHAPTER 5: CONCLUSIONS 79

5.1. Summary of Work Done 79

5.2. Conclusion 80

5.3. Future Work 80

REFERENCES 82

LIST OF TABLES

TABLE 2.1: Phase Directional Element Operating and Polarizing Quantities 13

TABLE 2.2: IEEE-1547-2018. V and F Ride-through Conditions 37

TABLE 2.3: PRC-024-2 Frequency Ride-through Conditions 39

TABLE 2.4: PRC-024-2 Voltage Ride-through Conditions 40

TABLE 4.1: Directional Element Settings 61

TABLE 4.2: Directional Element Results for Rf=0 and 1 p.u Pre-fault Power 62

TABLE 4.3: Directional Element Results for Rf=40 and 1 p.u Pre-fault Power 62

TABLE 4.4: Directional Element Results for Rf=40 and 0.5 p.u Pre-fault Power 62

TABLE 4.5: Directional Element Results with Modified Relay Logic for Rf=0 and 1 p.u Pre-fault Power 76

TABLE 4.6: Directional Element Results with Modified Relay Logic for Rf=40 and 1 p.u Pre-fault Power 76

TABLE 4.7: Directional Element Results with Modified Relay Logic for Rf=40 and 0.5 p.u Pre-fault Power 76

LIST OF FIGURES

FIGURE 2.1: Negative-Sequence Directional Element Interlocks 17

FIGURE 2.2: Type I WTG Typical Configuration 21

FIGURE 2.3: Type II WTG Typical Configuration 22

FIGURE 2.4: Type III WTG Typical Configuration 23

FIGURE 2.5: Type IV WTG Typical Configuration 24

FIGURE 2.6: General Synchronous Controller Structure 26

FIGURE 2.7: Basic Block Diagram of SRF-PLL 28

FIGURE 2.8: Basic Block Diagram of DSRF-PLL 29

FIGURE 2.9: Sequence Decoupling Method 32

FIGURE 2.10: Decoupled Sequence Current Controller 33

FIGURE 2.11: IEEE 1547-2018 HVRT/LVRT Curve 37

FIGURE 2.12: IEEE 1547-2018 OFRT/LFRT Curve 38

FIGURE 2.13: PRC-024-2 LFRT/OFRT Curve 40

FIGURE 2.14: PRC-024-2 HVRT/LVRT Curve 41

FIGURE 2.15: T-Capability Curve 41

FIGURE 2.16: Dynamic Reactive Current Requirement from German Grid Code 42

FIGURE 3.1: Two Traditional Sources Power System 45

FIGURE 3.2: Sequence Diagram for a Single Line to Ground Fault 45

FIGURE 3.3: V_2 and I_2 phasors for Forward and Reverse Faults 47

FIGURE 3.4: z_2 Magnitude and Thresholds for Forward and Reverse Faults 48

FIGURE 3.5: German Grid Code-based WPP Fault Behavior 51

FIGURE 4.1: Test System Single Line Diagram 54

FIGURE 4.2: Type-IV WPP Single Line Diagram 55

FIGURE 4.3: Coupled Control 56

FIGURE 4.4: AG Fault Results at Bus1 with Rf=0 ohms and 1 p.u Pre-fault Power for Three WPP Controls 63

FIGURE 4.5: V_2 and I_2 Phasors for AG Fault for Rf=0 ohms and 1 p.u Pre-fault Power 63

FIGURE 4.6: BC Fault Results for Rf=0 ohms and 1 p.u Pre-fault Power for the Three WPP Controls 64

FIGURE 4.7: V_2 and I_2 Phasors for BC Fault for Rf=0 ohms and 1 p.u Pre-fault Power 64

FIGURE 4.8: AG Fault Results for Rf=40 ohms and 1 p.u Pre-fault Power 65

FIGURE 4.9: AG Fault Results for Rf=40 ohms and 0.5 p.u Pre-fault Power 66

FIGURE 4.10: AG fault Vabc, Iabc Results for Rf=0 ohms for Conventional Source at Relay1 67

FIGURE 4.11: AG Fault Sequence Components Results for Rf=0 ohms for Conventional Source at Relay1 68

FIGURE 4.12: AG Fault Vabc, Iabc Results for Rf=0 ohms for German Grid Code-based WPP at Relay1 69

FIGURE 4.13: AG Fault Sequence Components Results for Rf=0 ohms for German Grid Code-based WPP at Relay1 70

FIGURE 4.14: AG Fault Results for Rf=40 ohms and 1 p.u Pre-fault Power for Three Controls at Relay1 with Modified Logic 75

LIST OF ABBREVIATIONS

BES Bulk Energy Resource

BPSC Balanced Positive Sequence Control

CC Coupled Control

CSI Current Source Inverter

DFIG Doubly-Fed Induction Generator

DR Distribution Resource

DSC Decoupled Sequence Control

DSRF PLL Decoupled Synchronous Reference Frame Phase Locked Loop

ECA (Directional) Element Characteristic Angle

ERCOT Electric Reliability Council of Texas

FERC Federal Energy Regulatory Commission

FPNSC Flexible Positive Negative Sequence Control

FRT Fault-Ride Through

GSC Grid Side Converter

HVRT High Voltage Ride Through

IARC Instantaneous Active Reactive Control

IBR Inverter Based Resource

IG Induction Generator

ISO Independent System Operator

LFRT Low Frequency Ride Through

LVRT Low Voltage Ride Through

MW Megawatt

N.O. Not Operated

NERC North American Electric Reliability Corporation

OFRT Over Frequency Voltage Ride Through

PLL Phase Locked Loop

PNSC Positive Negative Sequence Control

POTT Permissive Overreaching Transfer Trip

PWM Pulse Widthe Modulation

RTO Regional Transmission Organization

SRF PLL Synchronous Reference Frame Phase Locked Loop

STATCOM Static Compensator

VSI Voltage Source Inverter

WTG Wind Turbine Generator

CHAPTER 1: INTRODUCTION

1.1 Overview

This thesis is focused on improving the performance of the negative-sequence directional element for Type-IV wind power plants. Suitable fault ride-through conditions (FRT) are identified first and then shortcomings with that conditions are addressed by proposing four solutions. Two solutions are related to the fault ride-through (FRT) conditions and two solutions are related to the relay logic. The proposed techniques will enhance the dependability and security of the negative-sequence directional element.

This chapter is organized as follows. Section 1.2 provides the motivation for this work. Section 1.3 presents the literature review. The thesis problem statement is presented in Section 1.4. Section 1.5 presents the thesis overview and summary of research contributions. Finally, an overview of the thesis organization is presented in Section 1.5.

1.2 Motivation

Negative-sequence directional element gained more popularity with the advent of numerical relays due to its simplicity and high reliability for traditional sources compared to other available directional elements. But for the inverter-based resources (IBR) like wind power plants and solar power plants, this element is shown to have less reliability and now the power industry is searching for alternative and reliable solutions for directional elements[1]. This IBR megawatt share in the power system is also steadily increasing which requires immediate attention from the protection engineers.

Growing energy demand and the need to reduce carbon emissions are two strong propelling forces in the rapid increase of large-scale integration of renewable energy resources into the present energy industry [2]. Wind energy is the most viable solution for many countries to replace large-scale conventional fossil fuel energy. Government policies that are mandating and encouraging energy efficiency are another contributor to the development of new wind power technologies; one such development is the use of inverters in wind turbine integration to the grid. There is an on-going improvement in the wind manufacturing sector, and recently, Siemens-Gamesa has announced an offshore wind turbine, which can generate 14 MW from a single unit.

With the increase in IBR integration into the power system, traditional sources contribution requirement is coming down. When these resources are replacing conventional generators, they must play the role of conventional sources in maintaining the power system stability during fault conditions. Grid codes specify the voltage and frequency ride-through conditions (define how much time an IBR should be connected to the grid) as well as fault ride-through (FRT) conditions (how the IBR should behave during that time). Fast controls associated with the inverter can achieve these FRT conditions in the first few cycles following the fault inception. Protection engineers can take advantage of defined fault behavior in the control scheme, but this can only happen with comprehensive grid codes. Present North America grid codes are not comprehensive and do not specify any negative-sequence currents injection requirement from an IBR during FRT condition. Hence, protection engineers are facing challenges to develop common protection philosophies for the IBRs.

Protective relays are intelligent devices that can see the abnormality in the power system and act accordingly. Nevertheless, with these inverters, which are also intelligent enough to act so fast to reduce the fault currents and produce the defined control scheme, protective systems philosophies are in need to modify accordingly. There is a need to develop the protection functions based on the control system or otherwise,

controls are to be developed to have a similar fault behavior like a traditional source.

1.3 Literature Review

Introduction

The literature review part organized in the manner to present some of the published papers and textbooks, which are very much directly related to conducting the thesis work. This section presents various topics in a sequential manner. First, types of wind turbine generators and their fault characteristics related literature are presented. Next, Grid side converter control structures focusing majorly on phase-locked loop design and current control strategies, which can affect the fault behavior of the IBR. Then, traditional power system protection function philosophies and challenges to implement with IBR are discussed. Next, directional protection misoperation due to the presence of the wind power plant. Finally, practically feasible alternate protection function suggestions for the IBR to address some of the protection challenges.

Literature Review

Fault current contributions are not similar for various types of WTGs [3, 4]. Type-I and Type-II WTGs are induction generators with no converter controls. Their fault current contribution depends on the physical characteristics. Type-I and II WTG fault behavior can be analyzed using Thevenin's equivalent circuit representation which contains a voltage source in series with the (flux time constant based) impedance [4, 5]. Type-III WTGs are doubly-fed induction generators with back-to-back converters in the rotor circuit. Rotor circuit includes a crowbar feature to protect power electronic equipment from high currents generated in the rotor circuit during system fault conditions. One good thing is if crowbar is actuated, Type III fault behavior is just like a Type-II WTG, which can be analyzed using traditional methods. Unfortunately, crowbar operation is not continuous for intermediate severe faults and results in complex fault characteristics. Type-IV WTGs are permanent

magnet synchronous generators or induction generators with back-to-back converters on the stator side. Type-IV WTGs are full controlled converter-based resources with less complex fault characteristics than Type-III WTGs as there is no crowbar requirement. However, because of the manufacturer-specific fast inverter controls and as the fault currents are restricted to rated inverter currents, fault behavior for Type-IV WTGs is very different to traditional sources and cannot be analyzed using traditional short circuit tools [6].

Type-III and Type-IV WTGs fault current behavior is based on the converter control system design. There are several things to consider inside converter controls, which can affect the fault currents. Majority of this fault current signatures are due to FRT conditions defined in the converter control system and due to phase-locked loop (PLL) [7, 8], which is the key driving force for the control system. FRT conditions are defined based on grid codes, and if they are not covered, manufacturer can have a free hand in defining the control scheme.

Reference [9] explains the importance of positive-sequence voltage and phase angle accurate estimation, which is the duty of the phase-locked loops. Phase angle estimation is the key driving force for the converter control system which will be useful for synchronizing the converter to the grid and for the power calculations. Faults associate with sudden phase jumps and especially, unbalanced faults offer negative-sequence voltages which cause the double- frequency oscillations in the d and q voltage measurements [10]. Reference [9] also shows the approximation approach of synchronous reference frame PLL which filter out the high-frequency voltage signals resulting error in the phase angle measurement. The paper also proposes a method which is completely a mathematical approach to decouple the positive and negative-sequence synchronous reference frames voltage signals in such a way that positive-sequence rotating frame (dq) signals will be free from the negative-sequence rotating frame (dq) signals. By decoupling this way, accurate positive-sequence phase

angle measurement and positive-sequence voltage could be possible. In this approach, (DSRF) PLL can provide the decoupled positive-sequence reference frame d and q voltage components and negative-sequence reference frame d and q components which can be further utilized by the control system.

SRF-PLL uses bandwidth reduction technique to remove the harmonics or noise [11]. If this technique is used to remove the double- frequency oscillations in positive-sequence synchronous reference frame d and q components, it may result in less accurate phase angle measurement. Decoupled alpha-beta stationary reference frame PLL also follows this decoupling technique, and [7] shows the advantages that the method offered in reducing the frequency overshoot compared to DSRF-PLL, without compromising on the accuracy of the phase angle measurement. For severe fault conditions where the voltage of the power system goes very low, PLL may cause loss of synchronism or instability in the control system. One practical solution to avoid this situation is by freezing the PLL [12]. Freezing PLL may not address the changes that happened in frequency and phase angle. Reference [8] evaluated the robustness of the frozen PLL and compared that with an algorithm based phase compensated frozen PLL.

Reference [13] explains comprehensively about extracting the positive-sequence dq0 currents and negative-sequence dq0 currents by using park transformation method. This reference also comprehensively presented the current control strategies for power control under unbalanced grid conditions like instantaneous active−reactive control (IARC), positive-negative-sequence control (PNSC), average active−reactive control (AARC), balanced positive-sequence control (BPSC), flexible positive- and negative-sequence control (FPNSC). FPNSC explains that with the selection of a proper portion of positive-sequence and negative-sequence currents, it can mitigate the double-frequency active power or reactive power oscillations as per the requirement. BPSC strategy explains to achieve the balanced three-phase currents during balanced as well

as unbalanced grid conditions. This reference mentions average values of the active power and reactive power can be achieved by an infinite number of combinations of three-phase currents. There should be a specific strategy from an inverter control system to converge these three currents.

Reference [14] shows that IBR with a balanced current control strategy, offers high negative and zero-sequence impedances. Low fault currents in the range of normal operating currents are another contributor to the protection challenges. Because of these deviations, many protection philosophy deviations are observed. Negative-sequence directional element, faulted phase selection, fault location, incremental quantities, fault type detection, phase and ground over current elements and distance elements are among those affected protection functions. The reference addresses these deviations comprehensively for all the protections affected, which are mentioned above.

Reference [15] shows that negative-sequence directional element supervised over current relay misoperation when it is set to look towards a Type-IV WTG for two different cases. First, Type IV WTG with balanced current control strategy connected to a conventional source (two sources), developed in simulink software. Second, from the field relay recordings of a power plant with Type IV WTGs. In the second case, for a BCG fault, sequence phasor diagrams showed the small magnitude of negative-sequence current and phase angle conflict with respect to negative-sequence voltage, causing wrong directional decision. Balanced current control strategy of the WTG ensures balanced currents even during unbalanced fault conditions, which is the cause for the small magnitude of the negative-sequence current. WTG response is observed as if the negative-sequence currents are flowing in a traditional capacitive system (though the system is inductive). The traditional directional elements are set and expect inductive behavior of the power system. The paper suggests to change negative-sequence directional element line impedance (Z_{L2}) angle setting to counter the misoperation.

Reference [1] shows the recordings from the field relays for two different cases, 1st case with Type-III WTGs connected and second case with STATCOMs connected through full power converters. For both cases, there is a grounded transformer to connect these sources to the transmission line. From the relay recordings, it is observed that, for the faults associated with ground, zero-sequence current magnitude is high enough, and phase angle is consistent just like the traditional sources. In contrast, negative-sequence current magnitude is minimal in magnitude and phase angle with negative-sequence voltage is not consistent. Zero-sequence directional element operated correctly for the cases shown, and negative-sequence directional element misoperated. Grounded transformers being the zero-sequence current sources, and the converter control algorithm has no role on zero-sequence currents at the line side. Hence, zero-sequence directional element performance is expected to be similar to a traditional system. Reference [1] provided relay recordings, which showed proper zero-sequence directional element performance. Disadvantages from the zero-sequence directional element is that the fault should associate with ground, and this element is not immune to mutual coupling from nearby power lines [16]. Reference [1] also shows line current differential and POTT scheme with echo logic as alternative solutions for IBRs with low negative-sequence fault currents.

Reference [17] mentions, IBR fault current injection to the grid is quite different to conventional generators. Conventional protection functions operation and performance depend on the fault current phasors (includes magnitude as well as phase angle). IBR fault current phasors are not as expected from the many protection functions. IBR control algorithms are very fast, but they take at least one power cycle to detect the fault and act to control the fault current. Protection algorithms like incremental quantity detection and traveling wave detection schemes which can sense the faults within one cycle are seems to be promising for the IBR applications. The fact that traveling wave fault detection scheme operating principle relies on the char-

acteristic impedance of the line and independent of the connected sources is another factor that is raising the hope for reliable alternative protection.

1.4 Problem Statement

Protection functions should operate for the faults which are in the protection zone (dependability) and should restrain for the out of zone faults (security) [18]. These two, dependability and security, are part of reliability metrics and are very important to specify the performance of any protection element. Negative-sequence directional element is one of the protection functions which is suffering for these metrics when fault current is provided by the IBR.

This thesis's main objective is to analyze the negative-sequence directional element for the full-scale controlled (Type-IV) WPP with various control schemes and provide recommendations to enhance the performance of the directional element. Three different inverter control models developed in EMTP-RV are used to analyze the fault behavior of Type-IV WPP. This work uses average value models instead of detailed models. Reference [19] concludes on computational gain achieved without losing acceptable accuracy from average value models in comparison to detailed models (up to 50 μs time step).

The literature review part shows the negative-sequence directional element advantages in sensing the fault direction for traditional systems and shows the dependability and security issues with IBR. This work provides the inverter control system with a suitable FRT, and solutions for achieving the same dependability and security of this element for protecting the IBR, like it has in case of a traditional source. The research work shows that the German grid code-based control scheme has negative-sequence currents from the IBR, similar to an reactance dominated traditional source. This control system shows to be promising in solving the performance issues of the directional element. However, two problems are observed for this control system. First,

dependability issues for high impedance faults. Second, German grid code does not specify explicitly about I_2-active which is to be injected to the grid during FRT. The control model implemented in EMTP-RV assumes I_2-active as zero, which may not be the case with real-time IBR. If I_2-active is positive and if it is dominant compared to I_2-reactive, the negative-sequence phase angle will become small and could pose security issues for the directional element. This thesis work provides recommendations to counter these two problems associated with the German grid code-based IBR control system.

1.5 Thesis Overview and Research Contribution

This section presents the main objectives of this thesis work and research contributions for achieving the objectives.

Thesis overview

This thesis work analyzes negative-sequence directional element performance for three control schemes for Type-IV WPP. This work observes coupled control and decoupled sequence control-1 for Type-IV WPP are not providing consistent results. This work observes German grid code implemented Type-IV WPP (DSC-2) inverter control system negative-sequence currents are similar to the traditional sources. This thesis work shows German grid code implementation solves the challenges associated with the directional element to a certain extent. Furthermore, inverter control system must address a few things to overcome the dependability issues with high impedance faults. Otherwise, directional element should address these issues by modifying it's logic.

Research contributions

Four recommendations are given, which can further improve the performance of the directional element for the German grid code implemented Type-IV WPP. Two recommendations are for the inverter control system and two for the negative-sequence

directional element logic.

The proposed additional features from the control system

- The implementation of minimum $\frac{|I_2|}{|I_1|}$ by varying the k_{neg} (k multiplier for $|I_2|$) dynamically from 2 to 6 (minimum and maximum values for k).

- German grid code does not mention about I_2-active, and this value is expected to be zero or negative for proper performance of the directional element i.e. IBR should consume I_2-active during unbalanced fault conditions. Hence, the inverter control system should follow I_2-active as zero or some negative-value. This thesis work uses DSC-2 control, which implemented I_2-active as zero.

Alternative to the above points, The proposed modifications from the directional element logic are,

- Directional element logic may be modified by changing $\frac{|I_2|}{|I_1|}$ (a2 setting) to $\frac{|I_2-reactive|}{|I_1-reactive|}$, making the directional element a2 setting independent of the I_1-active current component.

- ECA setting may be modified from the transmission line angle ($\angle Z_{L2}$) to 90^0 to make the directional element independent of the I_2-active component.

Improved results after implementing a2 setting modification to the relay logic are presented in this thesis work.

1.6 Thesis Organization

The remaining chapters of this thesis are organized as follows. Chapter 2 presents a background on directional elements, types of WTGs and modeling background on grid side converter control. Chapter 3 presents the analysis of the short circuit behavior of two-traditional-source system and Type-IV short circuit behavior for various control schemes and then proposed directional element modification is discussed. Chapter 4 then describes the test system including control schemes developed in EMTP-RV,

then several fault data obtained from the Type-IV WPP average value models with different controls (coupled control, generic decoupled sequence control, and German grid code-based control developed in EMTP-RV software) are presented, which are then analyzed for negative-sequence directional element performance. Finally, Chapter 5 provides, conclusions, research contributions and future work.

CHAPTER 2: DIRECTIONAL ELEMENTS, WIND TURBINE GENERATORS AND THEIR CONTROLS

2.1 Overview

Traditional protection function philosophies are based on the traditional sources. Before applying these protection functions to the IBRs, understanding of some of the topics are essential. This chapter presents the required knowledge to perform this thesis.

This chapter is organized as follows; section 2.2 covers directional elements available and their working principle. Section 2.3 presents an overview of types of WTGs. Section 2.4 provides background on grid side controller modeling. Section 2.5 covers North America grid codes for distribution resources and bulk energy resources. Section 2.5 also presents German grid code details.

2.2 Various Directional Elements in Protection System

Power system faults are needed to be segregated as per the fault direction to increase the protection system security and selectivity. Directional elements control the over current elements and supervise the distance elements. Traditionally, the following are the available methods to identify the fault direction.

- Phase directional element (T_{Phase})
- Positive-sequence voltage polarized directional element (32P)
- Negative-sequence voltage polarized directional element (32Q)
- Zero-sequence directional element

  Zero-sequence voltage polarized zero-sequence directional element (32V)

External source current polarized zero-sequence directional element (32I)

Phase Directional Element

Phase directional element on each phase independently declares the fault direction. A-phase directional element uses the BC phase to phase voltage (quadrature) as the polarizing quantity and in the same way, B and C phase elements.

Table 2.1: Phase Directional Element Operating and Polarizing Quantities [20]

Phase	operating quantity	Polarizing quantity
A	I_A	$V_{polA} = V_{BC}$
B	I_B	$V_{polA} = V_{CA}$
C	I_C	$V_{polA} = V_{AB}$

Table 2.1 shows the operating quantities and polarizing quantities for each phase directional element. Following are the torque equations for phase directional elements [20],

$$T_A = |V_{BC}|.|I_A|.cos(\angle V_{BC} - \angle I_A) \tag{2.1}$$

$$T_B = |V_{CA}|.|I_B|.cos(\angle V_{CA} - \angle I_B) \tag{2.2}$$

$$T_C = |V_{AB}|.|I_C|.cos(\angle V_{AB} - \angle I_C) \tag{2.3}$$

Torque measured for equations (2.1), (2.2), (2.3) will be positive whenever the phase angle difference between quadrature voltage (polarizing quantity) and phase current (operating quantity) is 0^0 to $+/-90^0$ (1st and 4th quadrants) and negative for values between $+/-90^0$ to $+/-180^0$ (2nd and 3rd quadrants). Each of the three directional elements, declares direction based on their torque measurements. If the measured torque is positive, directional element declares forward fault, and if the measured torque is negative, directional element declares reverse fault.

Positive-sequence Voltage Polarized Directional Element (32P)

The positive-sequence directional element uses only one element which can cover all the three phases, this can avoid the race between the elements, which can happen in the previously discussed directional element.

Torque equation for this element [20],

$$T_{32P} = |3V_1|.|3I_1|.cos(\angle 3V_1 - (\angle 3I_1 + \angle Z_{L1})) \tag{2.4}$$

$V_1 --> $ Positive-sequence voltage

$I_1 --> $ Positive-sequence current

Z_{L1} $--> $ Positive-sequence line impedance angle

Operating quantity $--> 3I_1.1\angle Z_{L1}$

Polarizing quantity$--> 3V_1$.

To avoid misoperation due to small values of polarizing or operating quantities, torque measured is compared with a threshold torque, above this threshold value only directional element gives a decision.

If the measured torque from (2.4) is positive, directional element declares forward fault, and if the measured torque is negative, directional element declares reverse fault.

During three-phase faults at relay terminals, the directional element may not give any decision due to the lack of polarizing quantity. To avoid this situation positive-sequence voltage memory (which lasts a few cycles) is used as polarizing quantity [21].

Negative-sequence Voltage Polarized Directional Element (32Q)

For unbalanced faults, there are cases (reference [20]) where positive-sequence directional element is not operated satisfactorily and for those cases, negative- sequence or zero-sequence based directional elements shown positive results.

Traditional phase directional elements requires three directional elements to cover all fault types. However, with the use of a negative-sequence directional element, the number of directional elements required to cover all fault types reduces to two. Positive-sequence directional element covers balanced faults, and negative-sequence directional element covers all un-balanced faults.

Torque equation for a negative-sequence directional element [20],

$$T_{32Q} = |3V_2|.|3I_2|.cos(\angle(-3V_2) - (\angle 3I_2 + \angle Z_{L2})) \tag{2.5}$$

V_2 $--> $ Negative-sequence voltage

I2 $-->$ Negative-sequence current

$\angle Z_{L2}$ $-->$ Negative-sequence line impedance angle

Operating quantity $-->$ $3I_2.1\angle Z_{L2}$

Polarizing quantity$-->$ $-3V_2$.

If the measured torque from (2.5) is positive, directional element declares forward fault, and if the measured torque is negative, directional element declares reverse fault.

Equation (2.5) can be simplified as,

$$T_{32Q} = Re[3V_2.(3I_2.1\angle Z_{L2})^*] \tag{2.6}$$

Equation (2.6) is just an alternative representation of (2.5), and both delivers same torque values.

New Negative-sequence Directional Element (32Q)

Negative-sequence impedance is used here as an alternative to the torque to determine the fault direction [20].

$$z_2 = \frac{Re[V_2.(I_2.1\angle Z_{L2})^*]}{|I_2^2|} \tag{2.7}$$

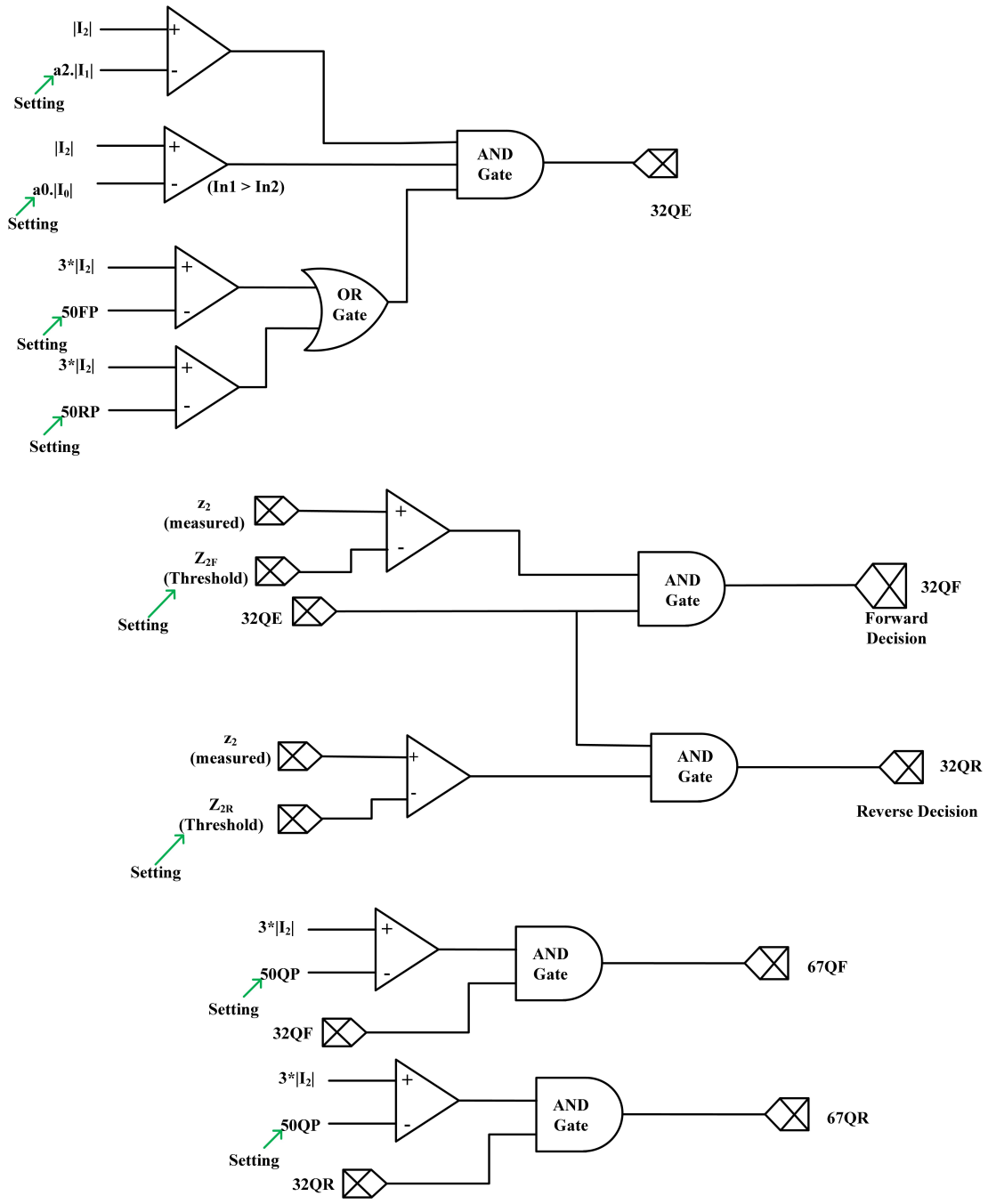

Figure 2.1: Negative-Sequence Directional Element Interlocks

The logic diagram for the negative-sequence directional element is shown in Fig. 2.1 [22]. Measured negative-sequence impedance (2.7) is compared to the forward and reverse threshold impedance values to determine the fault direction. In addition to the negative-sequence impedance threshold values, few other interlocks (a2, k2, 50FP and

50RP) are also to be satisfied to provide the fault direction by the negative-sequence directional element.

a2 setting: (positive-sequence restraint factor)

a2 setting decides the priority between the positive-sequence directional element and the negative-sequence directional element. If $|I_2|$ is less than a2 times of $|I_1|$, positive-sequence directional element gets the preference to decide the fault direction, and the negative-sequence directional element does not provide any directional decision.

k2 setting: (zero-sequence restraint factor)

k2 setting decides the priority between the zero-sequence directional element and the negative-sequence directional element. If $|I_2|$ is less than k2 times of $|I_0|$, zero-sequence directional element gets the preference to decide the fault direction, and the negative-sequence directional element does not provide any directional decision.

50FP/50RP (Negative-sequence minimum current setting):

Normal conditions like unbalanced loads or un-transposed transmission lines can have small negative-sequence currents. To distinguish these conditions from fault conditions and to restrain the directional element, 50FP/50RP settings are used in directional element logic. $3^*|I_2|$ should be higher than 50FP/50RP, only then this directional element provides fault direction.

Voltage Polarized Zero-sequence Directional Element

Faults involving ground allows to use this directional element in addition to other directional elements discussed. Torque equation for this directional element is analogous to negative-sequence directional element [20]. .

$$T_{32V} = |3V_0|.|3I_0|.cos(\angle(-3V_0) - (\angle 3I_0 + \angle Z_{L0})) \tag{2.8}$$

V_0 $--> $ Zero-sequence voltage

I_0 $--> $ Zero-sequence current

Z_{L0} $--> $ Zero-sequence line impedance angle

Operating quantity $--> 3I_0.1\angle Z_{L0}$

Polarizing quantity$--> -3V_0$.

Zero-sequence directional element (T32V) declares forward fault if the measured torque from the (2.8) is positive, and declares reverse fault if the measured torque is negative.

If the zero-sequence voltage is very small, which could be a possibility with strong zero-sequence sources (small neutral grounding impedance near the relay point), the phase angle between polarizing and operating quantities would be erratic and so the measured torque. For these type of systems (for the systems which can have low zero sequence voltages with ground faults), current polarized directional element is recommended.

Current Polarized Zero-sequence Directional Element

Here, polarizing quantity is current instead of zero-sequence voltage. phase angle difference between the current I_{op} and $3I_0$ decides the fault direction.

$$T_{32I} = |I_{pol}|.|3I_0|.cos(\angle(I_{pol}) - (\angle 3(I_0)) \tag{2.9}$$

The directional element declares forward fault, if the measured torque from (2.9) is positive, and declares reverse fault, if the measured torque is negative.

In addition to a2 and k2 settings, protection engineers are given the option to choose the priority within the elements negative-sequence voltage polarized element (32Q), zero-sequence voltage polarized element (32V) and zero-sequence current polarized (32I).

2.3 Types of Wind Turbine Generators

The principle of wind turbine operation is based on two well-known processes [23]:

- Conversion of the kinetic energy of moving air into mechanical energy using aerodynamic rotor blades and a variety of methodologies for mechanical power control.
- Electro-mechanical energy conversion through a generator that is transmitted to the grid.

Usually, wind turbines are classified by their mechanical power control and further by their speed control. All turbine blades convert the motion of air across the airfoils to torque and then regulate that torque to capture as much energy as possible.

Further wind turbines may be classified as either stall regulated or pitch regulated. Stall Regulation is achieved by shaping the wind turbine blades. The airfoil generates less aerodynamic force at high wind speed, eventually stalling, thus reducing the turbine's torque; this technique is simple, inexpensive, and robust. On the other hand, pitch regulation is achieved using pitching devices in the turbine hub, which twist the blades around their own axes. As the speed of wind increases, the blades quickly pitch to the optimum angle to control torque in order to capture the maximum energy or self-protect, as needed.

Types of Wind Turbine Generators:

- Type-I WTG: Squirrel cage induction generators
- Type-II WTG: Wound rotor induction generators with variable rotor resistance
- Type-III WTG: Doubly-fed induction generators with power electronic converters on rotor side
- Type-IV WTG: Wound rotor synchronous machines with power electronic converters on stator side

Type-I Wind Turbine Generator

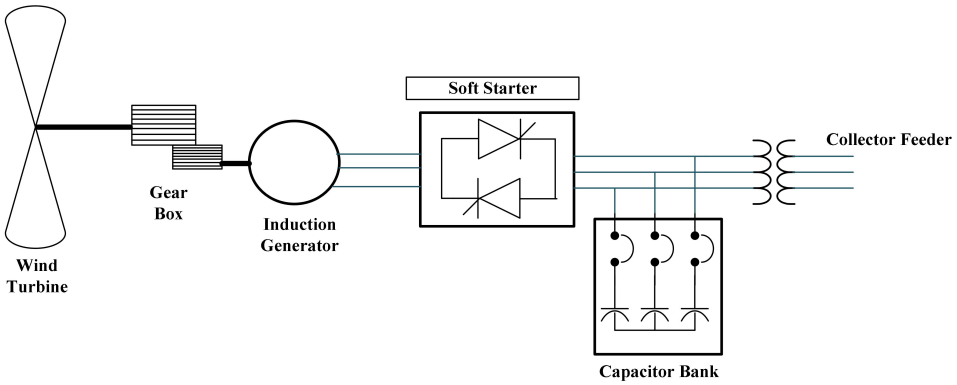

Figure 2.2: Type I WTG Typical Configuration

Type-I WTGs are squirrel-cage induction generators with a fixed speed, they are connected directly to the grid through a step-up transformer as shown in Fig. 2.2. Excitation support is taken from grid and power factor correction capacitor banks. Gearbox is used to increase the shaft speed by, typically, 100 times. Torque control is achieved by adjusting the pitch. The turbine speed is fixed (or nearly fixed) to the electrical grid frequency. It generates real power (P) when the turbine shaft rotates faster than the electrical grid frequency creating a negative slip (positive slip and power is motoring convention). For a given wind speed, the operating speed of the turbine under steady conditions is nearly a linear function of torque.

Type-II Wind Turbine Generator

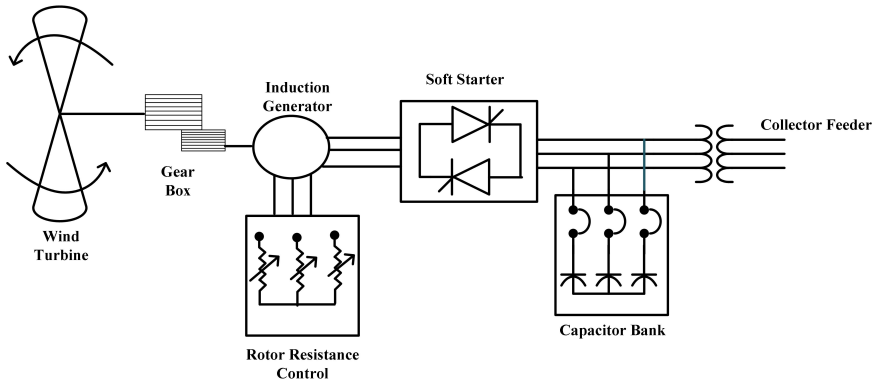

Figure 2.3: Type II WTG Typical Configuration

Type-II WTGs are wound rotor induction generators with variable speed, they are connected directly to the grid through a step-up transformer (Fig. 2.3) same fashion as Type-I WTGs. Excitation support is taken from grid and power factor correction capacitor banks. Variable rotor resistance implemented in the rotor circuit that can help in achieving the variable speeds (limited). Torque control is achieved by adjusting the pitch and/or rotor resistance.

Type-III Wind Turbine Generator

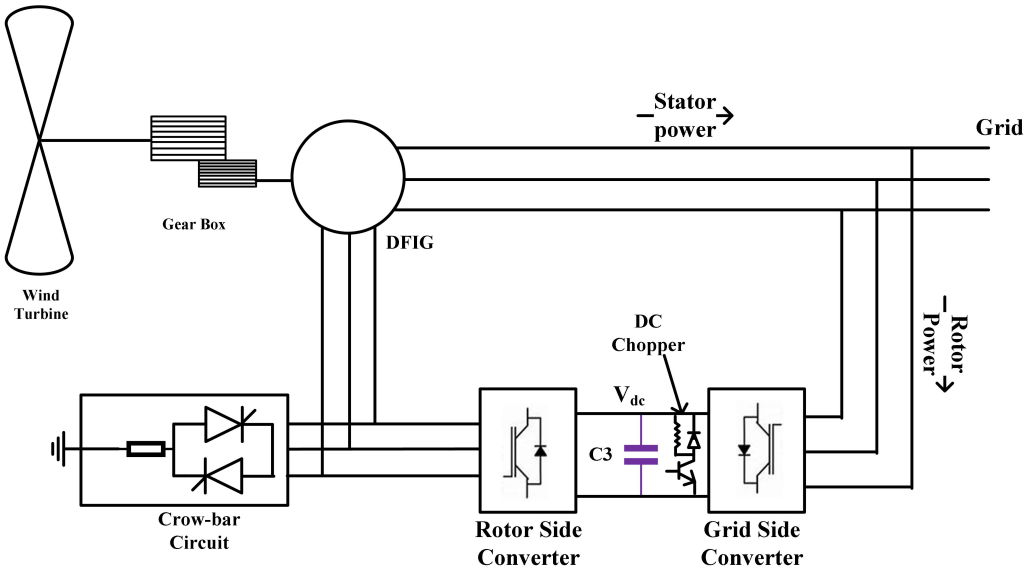

Figure 2.4: Type III WTG Typical Configuration

Type-III WTGs are doubly fed induction generators or doubly fed asynchronous generators. Rotor and grid side converters (back to back, connected by DC bus) are as shown in Fig. 2.4 . The rotor excitation supplied via slip rings by a current regulated voltage source converter. This rotor-side converter is connected back-to-back with a grid side converter, which exchanges power directly with the grid. Gearbox to increase shaft speed by, typically, 100 times. Crowbar circuit often used to short rotor windings after fault, and fault recovery based on the severity of the fault, to protect the rotor-side converter.

Type-IV Wind Turbine Generator

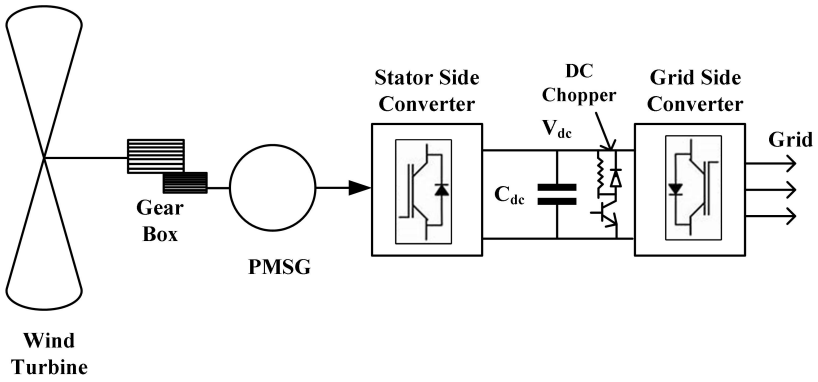

Figure 2.5: Type IV WTG Typical Configuration

Type-IV WTGs are again two types based on the excitation system, 1. Permanent magnet synchronous generators 2. Induction generators with machine side converter control for excitation requirement. Type 4 wind turbine offers a great deal of flexibility in design and operation as the output of the rotating machine is sent to the grid through a full-scale back-to-back converters as shown in Fig. 2.5. The turbine can rotate at its optimal aerodynamic speed and can still operate at the maximum power point. Besides, the gearbox may be eliminated, such that the machine spins at the slow turbine speed and generates an electrical frequency well below that of the grid.

2.4 Grid Side Controller Modelling Background

Introduction

Inverters broadly can be classified as voltage source inverters (VSI) and current source inverters (CSI). Usually, grid-connected sources use VSI and loads (like variable frequency drives) use CSI. VSI again divided into two types based on control methodology, current control mode, and voltage control mode. Voltage-controlled VSI active power and reactive power are controlled by regulating the voltage magnitude and voltage phase angle of the inverter output voltage with respect to the grid voltage [24]. On the other hand, current-controlled VSI active and reactive power injected into the grid are controlled using inverter output current phasors control.

Grid-connected sources controls happen at two levels: machine-side controller (MSC) and grid-side controller (GSC). MSC ensures operating the machine at the maximum power point, and GSC ensures the controlled power delivered to the grid with high quality in synchronization with the grid. GSC plays a crucial role in the fault behavior of full-scale converter-controlled sources.

In this section, a comprehensive background of three-phase grid-connected inverter is presented.

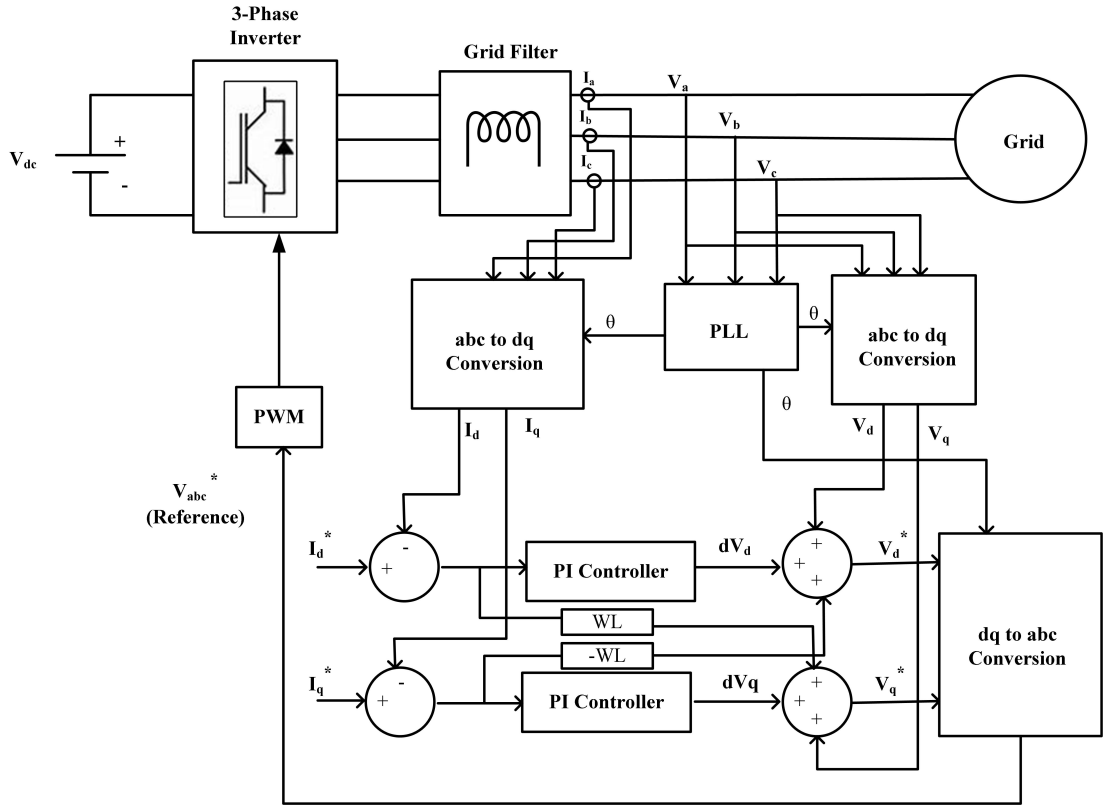

Figure 2.6: General Synchronous Controller Structure

Fig. 2.6 [25] presents an overview of a GSC control. GSC includes an inverter control system, collecting signals, extracting the phase angle, synchronizing power grids, carrying out abc to dq transform, calculating a reference current, controlling a current loop, carrying out dq to abc transform, controlling PWM and driving an inverter. Remaining sections of this chapter are focused on zooming inside this general structure.

2.4.1 Phase Locked Loop (PLL)

The inverter output voltage generated must be synchronized with the grid voltage all the time. Traditional synchronous generators once they are synchronized, they follow the grid. Whereas for an IBR connected to grid, it requires tracking and generation of synchronizing signal continuously for the inverter control system. The objective of the synchronization algorithm is to extract the phase angle and frequency

of the grid voltage. With the extracted grid phase angle, the measured signals are converted into corresponding synchronous reference frame (dq) signals, and in return, the phase angle again is used to convert the synchronous frame signals (dq) to time-domain three-phase signals. Generated dq signals are used as feedback signals for the inverter control system. Generated three-phase ac signal (Vabc*) is used to produce the switching pulses for the inverter switches. Hence, the detection of the grid phase angle plays an essential role in the control of the grid-connected inverter [5], [6]. The synchronization algorithms should respond quickly to changes in the utility grid and must provide fast and precise synchronization between the inverter and the grid. Furthermore, it must have a good response to harmonics, imbalances, phase jump, frequency changes, and various disturbing effects in grid voltages.

Many synchronization algorithms have been proposed to extract the phase angle of the grid voltage such as zero-crossing detection, and phase-locked loops (PLL). Nowadays, the most common synchronization algorithm for extracting the phase angle of the grid voltages is PLL. There are several PLL techniques available. Some of them are, manufacturers specific heuristic methods that are proprietary in nature.

Some of the PLL techniques are,

- Synchronous Reference Frame PLL (SRF-PLL)
- Decouple Synchronous Reference Frame PLL (DSRF-PLL)
- Stationary Reference Frame PLL ($\alpha\beta$-PLL) [26]

(This section restricted to discuss about synchronous reference frame based PLLs)

SRF-PLL:

SRF-PLL works by converting the stationary reference frame three-phase ac signals into two rotating signals, which are rotating at synchronous speed. Synchronous reference frame dq signals, looks like stationary signals with respect to each other.

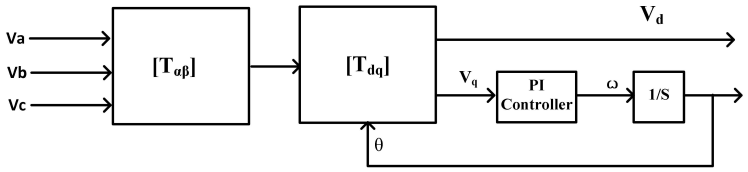

Figure 2.7: Basic Block Diagram of SRF-PLL

$$T_{dq} = \begin{bmatrix} cos\theta & sin\theta \\ -sin\theta & cos\theta \end{bmatrix} \tag{2.10}$$

The basic configuration of a SRF-PLL is shown in Fig. 2.7. Three-phase ac signals are converted into dq signals using the Park transformation method (2.10) [27]. The dq reference frame's angular position is estimated by a PI controller, which controls the V_q feedback signal by tracking it to zero.

SRF-PLL works satisfactorily for balanced grid conditions, i.e., when there is only one frequency component involved. If there is any noise or harmonics, the SRF-PLL response gets distorted and delayed. During unbalanced system conditions, a three-phase voltage signal contains a negative-sequence component. Though this negative-sequence signals rotate at the fundamental frequency, its rotating direction is opposite to positive-sequence signals. So synchronous reference frame signals contain two reference frames, positive-sequence reference frame and negative-sequence reference frame. The relative speed between these signals is double the fundamental frequency. This way, Positive-sequence reference frame dq signals contain double-frequency signals. If SRF-PLL considers only positive-sequence rotating frame signals and the PI controller if it tries to make q component to zero which is fluctuating with double the fundamental frequency, results in distortion in phase angle measurement.

Decoupled Synchronous Reference Frame PLL (DSRF-PLL):

DSRF-PLL is an improved version of a SRF-PLL. This PLL has positive-sequence rotating frame dq signals, and negative-sequence rotating frame dq signals. Reference

[9] shows proper mathematical decoupling of one's effect on another such that two mutually independent dq signals are achieved.

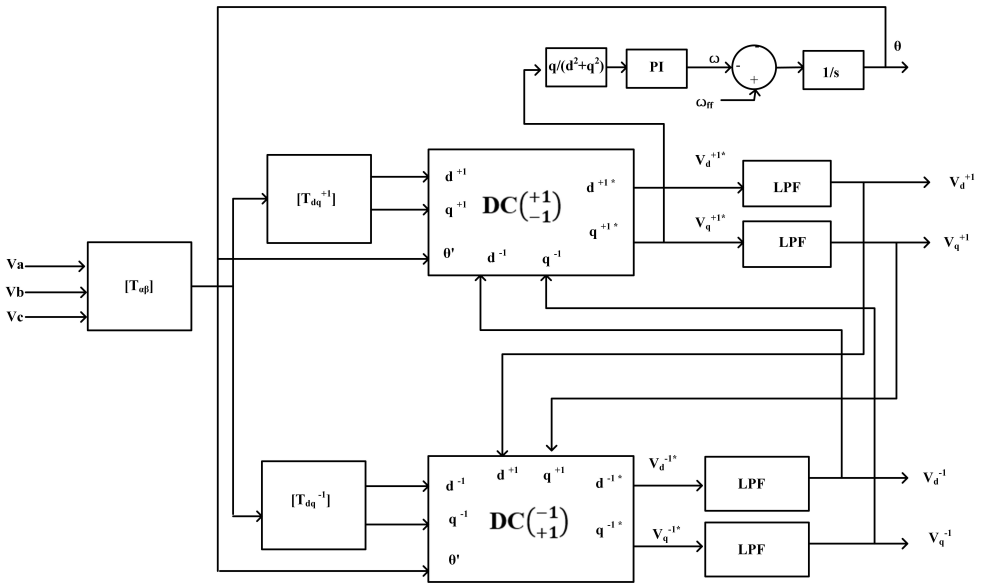

Figure 2.8: Basic Block Diagram of DSRF-PLL

Fig. 2.8 shows negative-sequence dq signals which are used as inputs for positive-sequence system.

$$V_{dq}^{+1} = \begin{bmatrix} V_d^{+1} \\ V_q^{+1} \end{bmatrix} = \left[T_{dq}^{+1}\right].V_{\alpha\beta} = V^{+1}.\begin{bmatrix} +1 \\ 0 \end{bmatrix} + V^{-1}.\begin{bmatrix} \cos(-2wt) \\ \sin(-2wt) \end{bmatrix} \tag{2.11}$$

$$V_{dq}^{-1} = \begin{bmatrix} V_d^{-1} \\ V_q^{-1} \end{bmatrix} = \left[T_{dq}^{-1}\right].V_{\alpha\beta} = V^{+1}.\begin{bmatrix} \cos(2wt) \\ \sin(2wt) \end{bmatrix} + V^{-1}.\begin{bmatrix} +1 \\ 0 \end{bmatrix} \tag{2.12}$$

$$DC\begin{bmatrix} +1 \\ -1 \end{bmatrix} = \begin{bmatrix} -cos2\theta & -sin2\theta \\ sin2\theta & -cos2\theta \end{bmatrix} \tag{2.13}$$

$$DC\begin{bmatrix} -1 \\ +1 \end{bmatrix} = \begin{bmatrix} -cos2\theta & sin2\theta \\ -sin2\theta & -cos2\theta \end{bmatrix} \tag{2.14}$$

$$V_{dq}^{+1} = \begin{bmatrix} V_d^{+1} \\ V_q^{+1} \end{bmatrix} + DC \begin{bmatrix} +1 \\ -1 \end{bmatrix} * \begin{bmatrix} V_d^{-1} \\ V_q^{-1} \end{bmatrix} \tag{2.15}$$

$$V_{dq}^{-1} = \begin{bmatrix} V_d^{-1} \\ V_q^{-1} \end{bmatrix} + DC \begin{bmatrix} -1 \\ +1 \end{bmatrix} * \begin{bmatrix} V_d^{+1} \\ V_q^{+1} \end{bmatrix} \tag{2.16}$$

$$[T_{dq}^{+1}] = [T_{dq}^{-1}]^T = \begin{bmatrix} cos\theta & sin\theta \\ -sin\theta & cos\theta \end{bmatrix} \tag{2.17}$$

Before decoupling, equation (2.11) shows a negative-sequence term in positive-sequence dq equation with double the frequency. If a double-frequency filter is used to remove this 2ω term, it will result in less accurate positive-sequence dq measurement and less accurate phase angle estimation. The decoupling network removes this 2ω term without losing any accuracy. Hence, wholly decoupled positive-sequence dq signals are available for the control system. Same with the negative-sequence dq signals (2.12).

Equations (2.13), (2.14), (2.15) and (2.16) explains the decoupling network working. Equation (2.17) shows park transformation for positive-sequence and negative-sequence reference frames. Once the decoupled positive-sequence voltage dq signals are obtained, the SRF-PLL technique is used to obtain the positive-sequence phase angle. This way, accurate phase angle measurement is achieved. Decoupling eliminates the second harmonic frequency term in d and q components, and helps in improved controller response due to reduced q component oscillations.

2.4.2 Three-phase Current Control Strategy

In this section, coupled sequence current control technique and decoupled sequence current control techniques are discussed.

Unbalanced grid conditions result in positive and negative-sequence voltages. Whereas,

positive and negative-sequence currents depends majorly on the inverter control system. Current-controlled VSI control system defines three-phase currents that are to be injected into the grid. Possible three-phase current combinations can be several for the same average active and reactive power. However, these current combinations can be reduced to two values, by expressing phase currents as positive-sequence currents and negative-sequence currents. Here, there can be two options, one, controlling only positive-sequence currents generally known as coupled control, second, controlling positive as well as negative-sequence currents generally known as decoupled sequence control. Coupled control does not control negative-sequence currents, hence ideally, it should not have any negative-sequence currents. Whereas, decoupled sequence current control generates negative-sequence currents based on the control objective.

Coupled Control

Fig. 2.6 also shows the coupled control technique (just the current control part). This control is straightforward. Natural reference frame abc currents are converted to dq signals (no decoupling). Current references are generated based on the control objectives like dc voltage control, active power, reactive power, etc. These d and q current references generates error signals against d and q current measurements (refer current control part of Fig. 2.6). These error signals goes to feed forward control (V_d, V_q measurements directly added to error signal) loops for generating Vabc reference (this part discussed later). There can be negative-sequence currents injected to the grid, as Coupled control is not controlling negative-sequence currents. In that case, there will be double-frequency oscillations in the dq current measured signals. This even results in active and reactive power oscillations.

Decoupled Sequence (Decoupled Double Synchronous Reference Frame) Current Control

Decoupled sequence current control has the control references for positive-sequence currents and negative-sequence currents. This way, this control model has complete control on the negative-sequence currents that are injected into the grid during fault conditions. Based on the control objective, these sequence current references change, and the control system guarantees these current references.

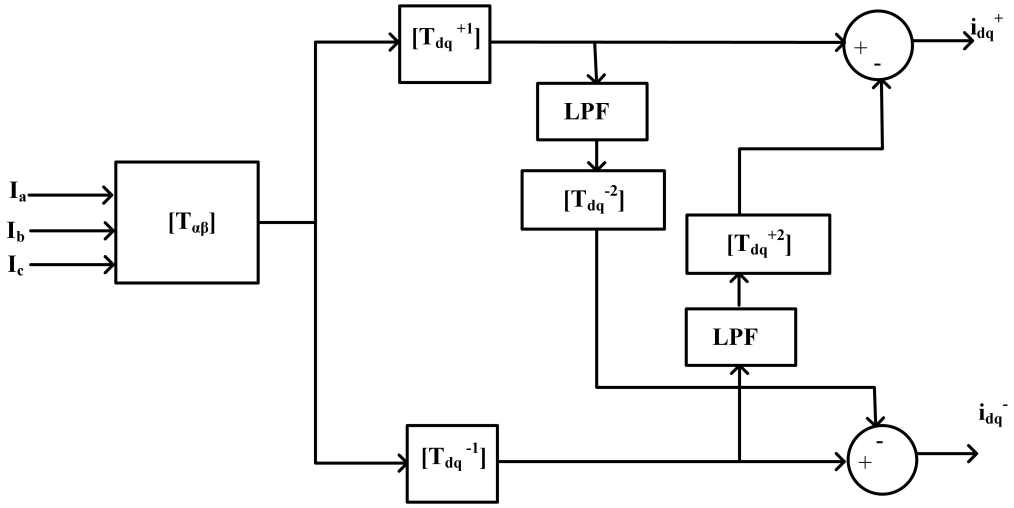

Figure 2.9: Sequence Decoupling Method

T_{dq}^{+1}–> Park transform matrix in positive-sequence synchronous reference frame

T_{dq}^{-1}–> Park transform matrix in negative-sequence synchronous reference frame

T_{dq}^{+2}–> double Park transform matrix in positive-sequence reference frame

T_{dq}^{-2}–> double Park transform matrix in negative reference frame

Fig. 2.9 shows the decoupling method for currents. This is same as explained in DSRF-PLL. The only difference is that the DC matrix is shown as double park transformation matrix (both are same) [13], and i_q^+ is not tracked to zero (PLL tracks v_q^+ signal to zero).

The output of this sequence decoupling network gives decoupled positive and negative-sequence d and q components. Once this four current signals (i_d^+, i_q^+, i_d^-

and i_q^-) are available, they can be used in independent control of each component.

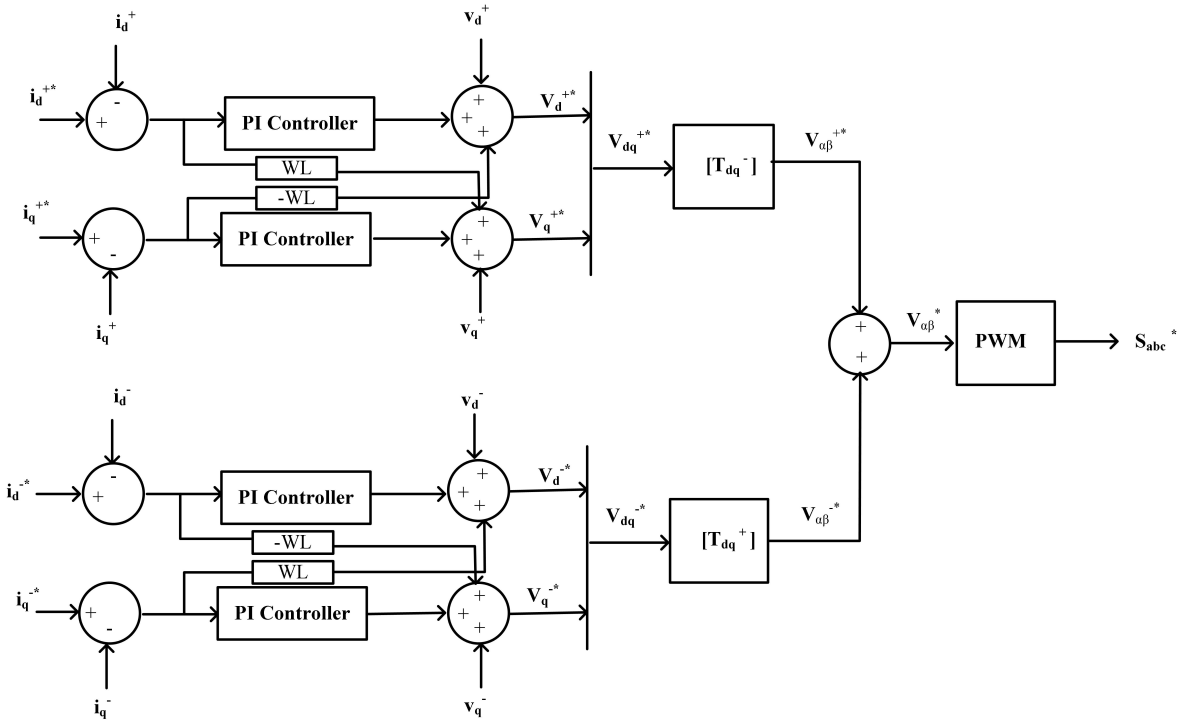

Figure 2.10: Decoupled Sequence Current Controller

Fig. 2.10 shows the current control structure of the GSC based on the decoupled double synchronous reference frame. Current reference generation is based on the current control strategy, and it varies from manufacturer to manufacturer.

Once four i_d^{+*}, i_q^{+*}, i_d^{-*} and i_q^{-*} reference currents are generated, four independent PI controllers are used to achieve these references against measured current signals i_d^+, i_q^+, i_d^- and i_q^-. Properly tuned PI controllers ensure the current references. Error signals that are generated in the process moves to feed forward control loop to generate Vabc reference.

2.4.3 Grid Filter Modelling

The grid filter is responsible for pure sinusoidal current signals from the PWM controlled inverter to the grid.

Mathematical modeling of RL-filter in synchronous reference frame:

Voltage drop due to inductance of RL-filter are shown in (2.18) and (2.19)

$$V_{dL} = -\omega * L * I_q \tag{2.18}$$

$$V_{qL} = \omega * L * I_d \tag{2.19}$$

Voltage drop due to resistance of RL-filter are shown in (2.20) and (2.21)

$$V_{dR} = R * I_d \tag{2.20}$$

$$V_{qR} = R * I_q \tag{2.21}$$

2.5 Grid Codes

Introduction

With the increase in IBR there is a need to keep these sources connected with the grid even in fault conditions. As such, there is no common grid code that applies to all territories in North America [28]. The North American Electric Reliability Corporation (NERC) has four isolated interconnection territories: Western, Eastern, ERCOT (Electric Reliability Council of Texas), and Quebec Interconnections. Besides, there are nine independent system operators (ISOs): Alberta, Ontario, Midcontinent, Southwest Power Pool, California, PJM Interconnection, ERCOT, New York, and New England.

NERC enforces standards that apply to voltage and reactive power control to ensure reliable operation. In the order 661A the Federal Energy Regulatory Commission (FERC) lays down site-specific reactive power requirements for TSOs that must be followed by site-specific wind farms. The ISO/RTO (Regional Transmission Organization) stipulates grid specific requirements such as low voltage ride-through, voltage regulation, reactive power control, and dynamic reactive power requirements. In addition to these requirements, a local utility may specify its interconnection requirements.

Distribution resources (DRs) connected to the distribution system are governed by IEEE Std. 1547 and bulk energy system resources (BES) connected to transmission system are governed by NERC reliability standards. NERC defines the resources, whether they are DRs or BES resources. Some of the NERC reliability standards for BES resources are PRC 024-2 which defines voltage and frequency ride-through, FERC Order 842 defines active power and frequency requirements, FERC order 827 specifies reactive power and Voltage requirements etc.

Broadly we can categorize these standards into static and dynamic requirements, static requirements related to the steady-state operating conditions (general require-

ments and power quality) and dynamic requirements related to the temporary behavior of the resources like abnormal system conditions and island conditions. In this section, focus has been given to the dynamic requirements of the IBRs.

2.5.1 Standards for Distribution Resources

2.5.1.1 IEEE Std. 1547-2018

IEEE 1547-2003 did not make any mandatory requirements for DERs related to ride-through conditions for voltage and frequency conditions. Seventeen years back, DR contributions to the power system were small, and DRs are sparsely located. As a result, the 2003 standard's philosophy centered largely around ensuring that DRs did not interfere with the normal operation of the distribution system regulation and protection systems. The standard specifies 'Cease to Energize' for abnormal voltage and frequencies in the system where DRs are connected.

IEEE 1547-2018 [29] increased its scope making some mandatory ride-through conditions, and it also specifically disallows voltage tripping within continuous operating region. It also increased the voltage range and clearing times for 'Cease to Energize' conditions for ensuring the DR to be in service for the remote faults and short-lived abnormal conditions.

DRs are again separated into three operating categories for abnormal conditions such as Category I, II, and III for defining the voltage range and clearing times.

Category I: is intended to meet minimum BES reliability and to be achievable by all DR technologies, including rotating machines.

Category II: is designed to align with the requirements in NERC PRC-024-2.

Category III: is designed to meet the needs of low-Inertia or highly penetrated grids, and to align with California rule 21, Hawaii rule 14, and similar rules.

Table 2.2: IEEE-1547-2018. V and F Ride-through Conditions [29]

	Category1		Category2		Category3	
	Pick-up(p.u)	Time(s)	Pick-up(p.u)	Time(s)	Pick-up(p.u)	Time(s)
OV2	1.2	0.16	1.2	0.16	1.2	0.16
OV1	1.1	2.0	1.1	2.0	1.1	13
UV2	0.7	2.0	0.7	2.0	0.88	21
UV1	0.45	0.16	0.45	0.16	0.5	0.2
OF2	62	0.16	62	0.16	62	0.16
OF1	61.2	300	61.2	300	61.2	300
UF2	58.5	300	58.5	300	58.5	300
UF1	56.5	0.16	56.5	0.16	56.5	0.16

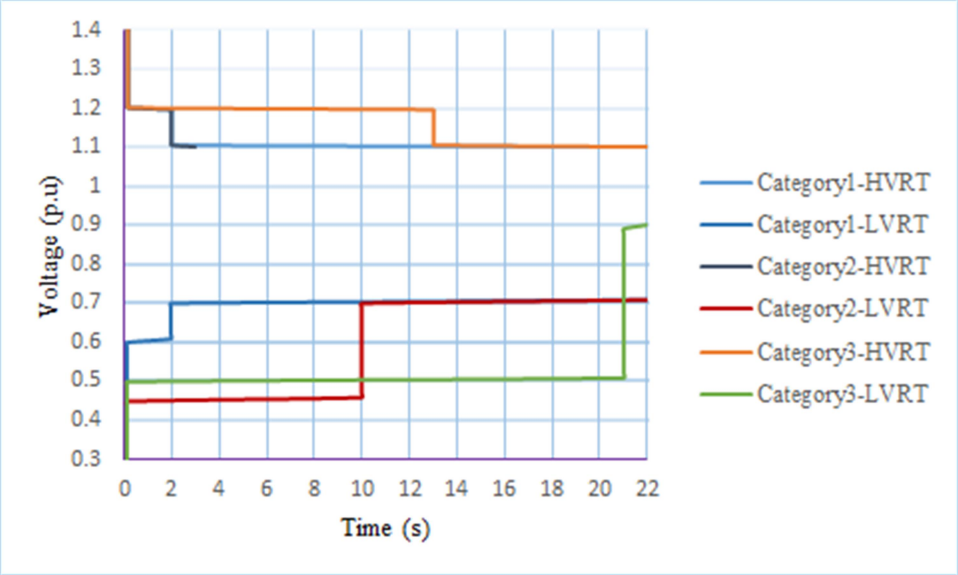

Figure 2.11: IEEE 1547-2018 Voltage Ride-through (HVRT/LVRT) Curve [29]

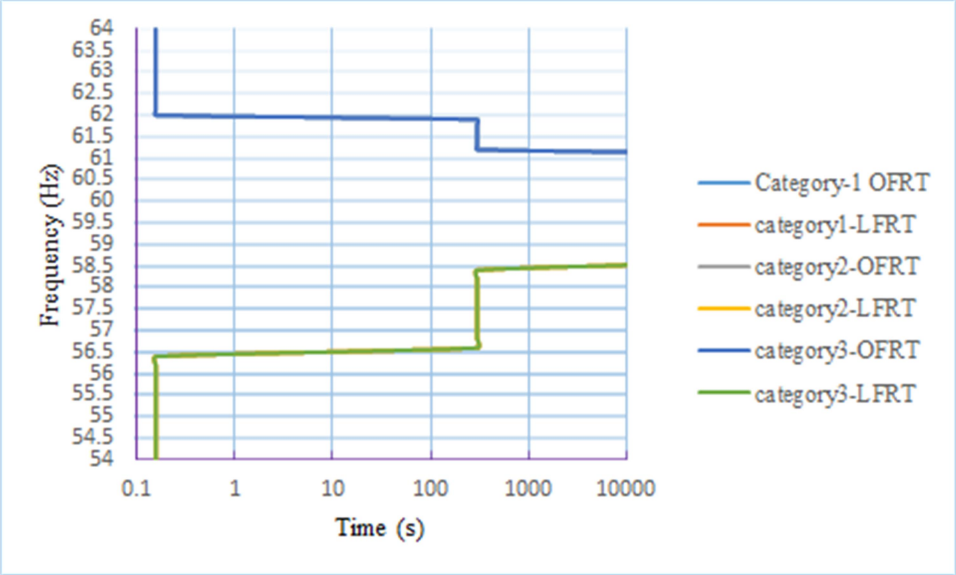

Figure 2.12: IEEE 1547-2018 Frequency Ride-through (OFRT/LFRT) Curve [29]

Table 2.2, Fig. 2.11 and Fig. 2.12 provides the IEEE 1547-2018 specified voltage and frequency ride-through conditions.

2.5.2 Standards for BES Connected Resources

2.5.2.1 Standard PRC-024-2

Table 2.3: PRC-024-2 Frequency Ride-though Conditions [30]

High Frequency Ride-Through

Frequency (Hz)	Time (s)
>=61.7	instantaneous trip
>=61.6	30
>=60.6	180

Low Frequency Ride-Through

Frequency (Hz)	Time (s)
<=57	instantaneous trip
<=57.3	0.75
<=57.8	7.5
<=58.4	30
<=59.4	180

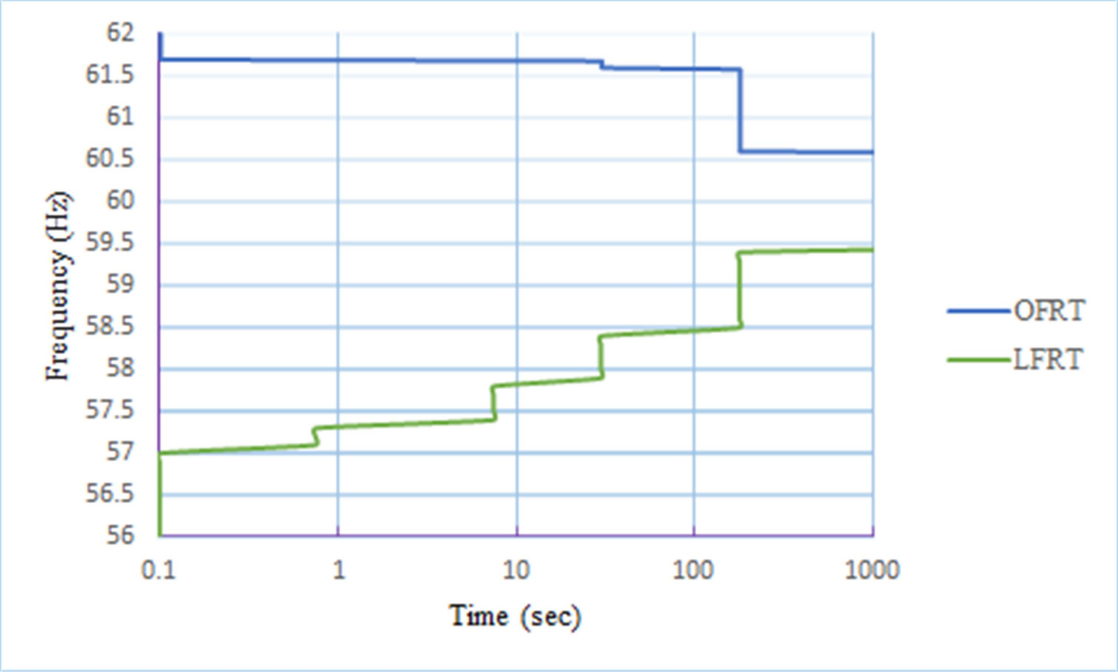

Figure 2.13: PRC-024-2 Frequency Ride-through Curve [30]

Table 2.4: PRC-024-2 Voltage Ride-through Conditions [30]

High Voltage Ride-Through

Voltage (p.u)	Time (s)
>1.2	instantaneous trip
>1.175	0.2
>=1.15	0.5
>=1.1	1

Low Voltage Ride-Through

Voltage (p.u)	Time (s)
<0.45	0.15
<0.65	0.3
<0.75	2
<0.9	3

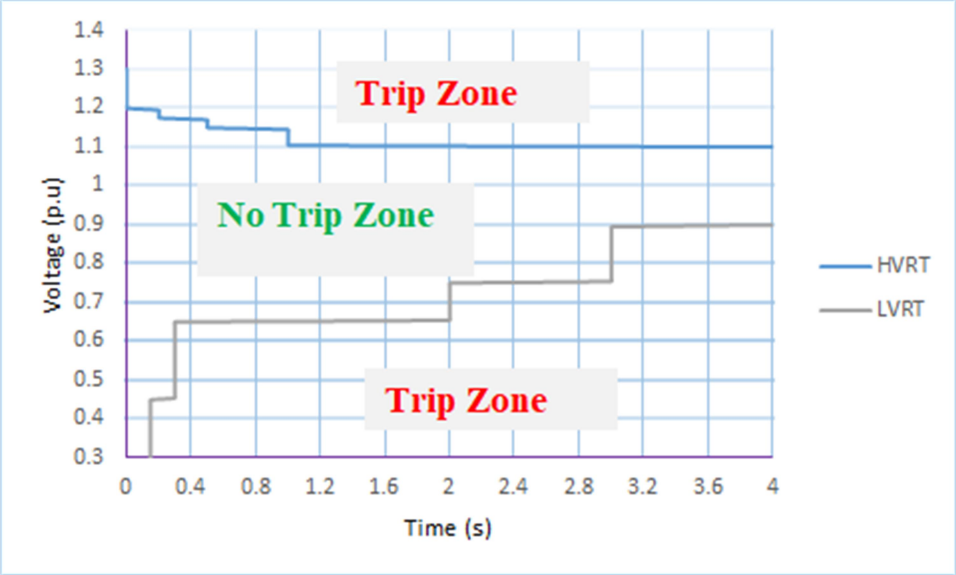

Figure 2.14: PRC-024-2 Votage Ride-through (HVRT/LVRT) Curve [30]

Table 2.3 and Fig. 2.13 provides frequency-ride through conditions mentioned in the PRC-024-2. Table 2.4 and Fig. 2.14 provides the voltage ride-through conditions mentioned in the PRC-024-2.

2.5.2.2 FERC Order 827 (Reactive Power-Voltage control)

This standard specifies, reactive power requirements during normal operating conditions,

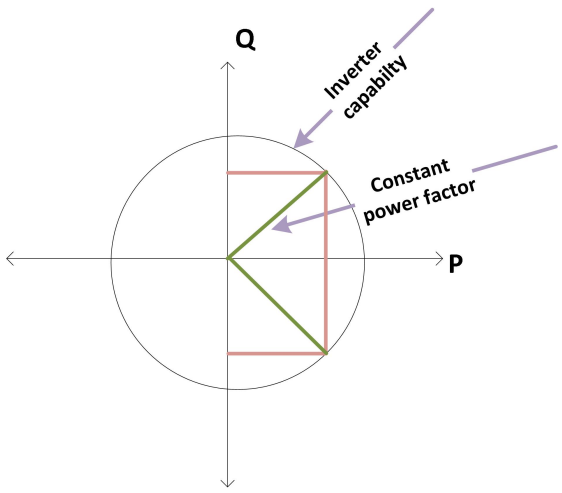

Figure 2.15: Triangle shaped Capability Curve

As per this standard, all newly interconnecting non-synchronous generators should be able to maintain the power factor between 0.95 leading to 0.95 lagging at all active power outputs. As per the example provided by FERC, 100 MW generator required to provide 33 MVAR at 100 MW output and 3.3 MVAR at 10 MW output (T-shape capability) Fig. 2.15.

2.5.2.3 NERC VAR 002 standard

This standard specifies, generators should operate in an automatic voltage control model at the point of interconnection. The generators should not restrict to FERC 827 order (T-Capability) during voltage deviations, instead they should operate based on the inverter current capability (semi-circle in Fig. 2.15).

2.5.3 VDE-AR-N 4120 (German Grid Code)

This standard specifies, dynamic grid support requirement in the form of positive and negative-sequence reactive currents. This dynamic reactive current requirement maintains the voltage stability and reduces the voltage surges in healthy phases [31].

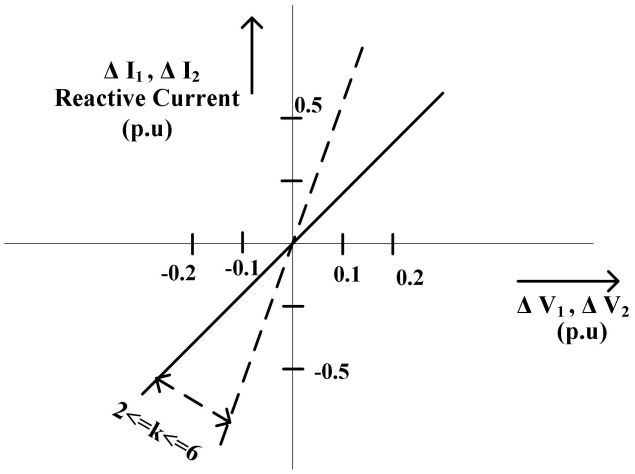

Figure 2.16: Dynamic Reactive Current Requirement from German Grid Code [31]

$$\frac{dI_{1reactive}}{dV_1} = \frac{dI_{2reactive}}{dV_2} = k \tag{2.22}$$

Fig. 2.16 shows the k-factor or slope between positive-sequence and negative-sequence reactive currents and their corresponding voltage change. Equation 2.22 also shows the same relation but in equation form. V1 and V2 are positive-sequence and negative-sequence voltages at the point of measurement (at the inverter terminal). The network operator conducts interconnection studies and specifies k-value for an IBR. This value generally varies from 2 to 6.

CHAPTER 3: ANALYSIS OF DIRECTIONAL ELEMENT APPLICATION FOR TRADITIONAL SOURCES AND TYPE-IV WIND POWER PLANTS

3.1 Overview

Understanding negative-sequence directional element function for protecting the traditional system is vital before analyzing it for Type-IV WPPs. This chapter is organized to present the short circuit behavior of traditional sources during unbalanced fault conditions. The directional element application part to the traditional sources shows how the negative-sequence currents and voltages relate to each other and how the directional element exploits this relation in deciding the fault direction. Then, Type-IV WPP short circuit behavior is discussed. Later, Type-IV WPP with German grid code is explained to show how it behaves during unbalanced fault conditions. Then, Type-IV WPP with this German grid code short circuit behavior is compared with the traditional source short circuit behavior. Finally, proposals to the relay logic are presented to improve the directional element performance for the Type-IV WPPs.

3.2 Traditional Sources Short Circuit Behavior

Controls of traditional sources are slow and do not play a role during the first few cycles of fault occurrence, and the fault currents are injected based on the physical characteristics of the generator. Rotating generators do not generate any negative-sequence voltages in general. During unbalanced fault conditions, fault point acts like a negative-sequence voltage source, as maximum unbalance persists at the fault point. Negative-sequence currents flow based on the impedance from fault point to source. The negative-sequence diagram can be represented with a series R-L circuit representing sources, transmission lines, and cables as R and L components [21]. This

R and L representation of the negative-sequence diagram is the key to applying the directional element for a traditional source. The following equations give analysis on the basics of the negative-sequence directional element application to a traditional source.

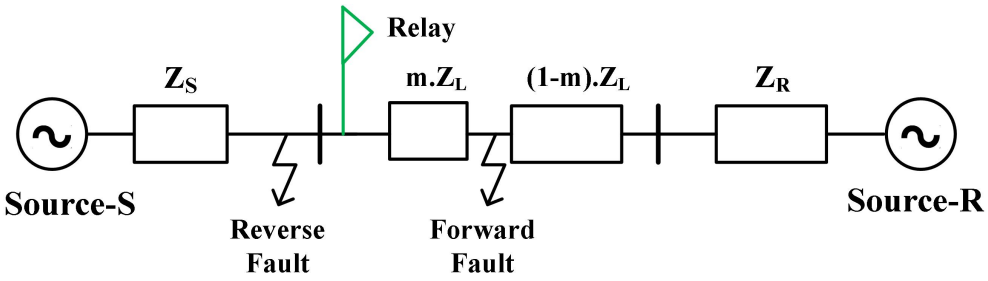

Figure 3.1: Two Traditional Sources Power System

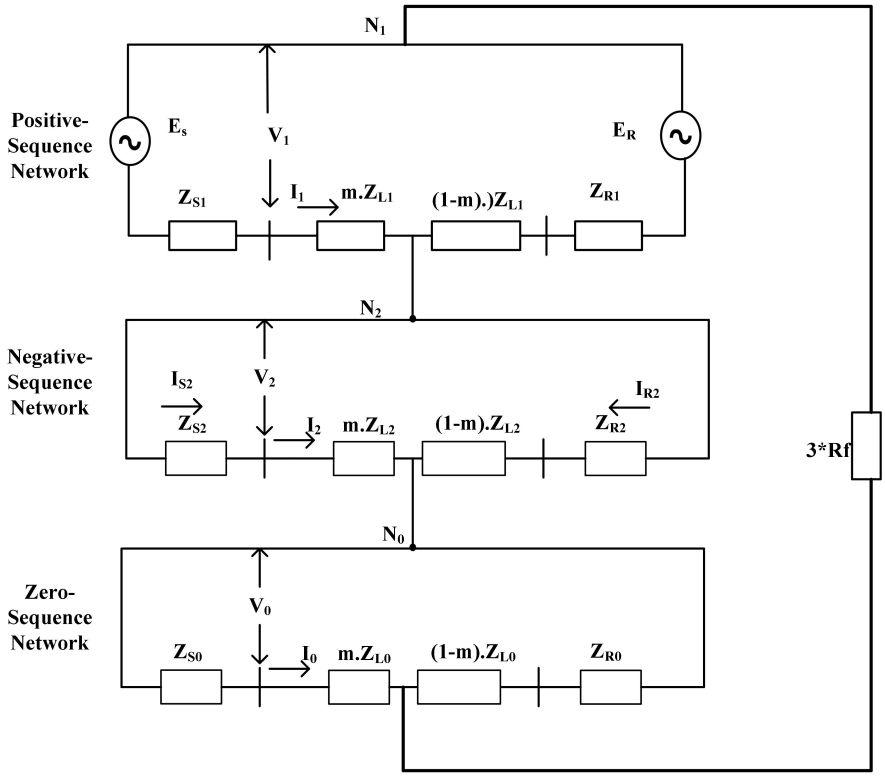

Figure 3.2: Sequence Diagram for a Single Line to Ground Fault

z_2 at relay point can be calculated from V_2, I_{S2} and I_{R2} as shown below,

For forward faults,

$$z_2 = \frac{-V_2}{I_{S2}} = -Z_{S2} \tag{3.1}$$

For reverse faults,

$$z_2 = \frac{-V_2}{-I_{R2}} = Z_{L2} + Z_{R2} \tag{3.2}$$

Two traditional sources connected with a transmission line is shown in Fig. 3.1. Relay is placed at one end of the transmission line. Forward and reverse faults are applied, as shown in the figure. Relay measures voltages and currents and converts them to sequence components. Relay calculates z_2, as shown in equation(2.7).

Equations (3.1) and (3.2) shows how the magnitudes of the negative-sequence impedance seen by the relay are varying for forward and reverse faults.

Negative-sequence network being series RL circuit as shown in Fig. 3.2, we can apply the following equations to calculate negative-sequence active and reactive power at the relay point (where V_2 is measured) for forward and reverse faults.

For forward fault,

$$P_2 = \frac{-3 * V_2^2 * R_{S2}}{R_{S2}^2 + X_{S2}^2} \tag{3.3}$$

$$Q_2 = \frac{-3 * V_2^2 * X_{S2}}{R_{S2}^2 + X_{S2}^2} \tag{3.4}$$

For reverse fault,

$$P_2 = \frac{3 * V_2^2 * (R_{L2} + R_{R2})}{(R_{L2} + R_{R2})^2 + (X_{L2} + X_{R2})^2} \tag{3.5}$$

$$Q_2 = \frac{3 * V_2^2 * (X_{L2} + X_{R2})}{(R_{L2} + R_{R2})^2 + (X_{L2} + X_{R2})^2} \tag{3.6}$$

P_2 and Q_2 values directly alter the angle between V_2 and I_2. Hence, equations (3.3), (3.4), (3.5) and (3.6) provide the fault direction, and shows the phase angle between V_2 and I_2 dependency on system R and L conditions.

For a negative-sequence directional element, z_2 impedance magnitude and V_2-I_2 phase angle relation is important in deciding the fault direction. As shown in Fig. 3.3, phasor positions of the V_2 and I_2 are actually reflected in (3.7) in deciding the fault direction. Understanding these phasor positions for forward and reverse faults

are having significance while analyzing the results with various IBR controls.

$$z_2 = Re(\frac{V_2 * (I_2.1\angle Z_{L2})^*}{|I_2^2|}) \tag{3.7}$$

3.2.1 Application of Negative-Sequence Directional Element

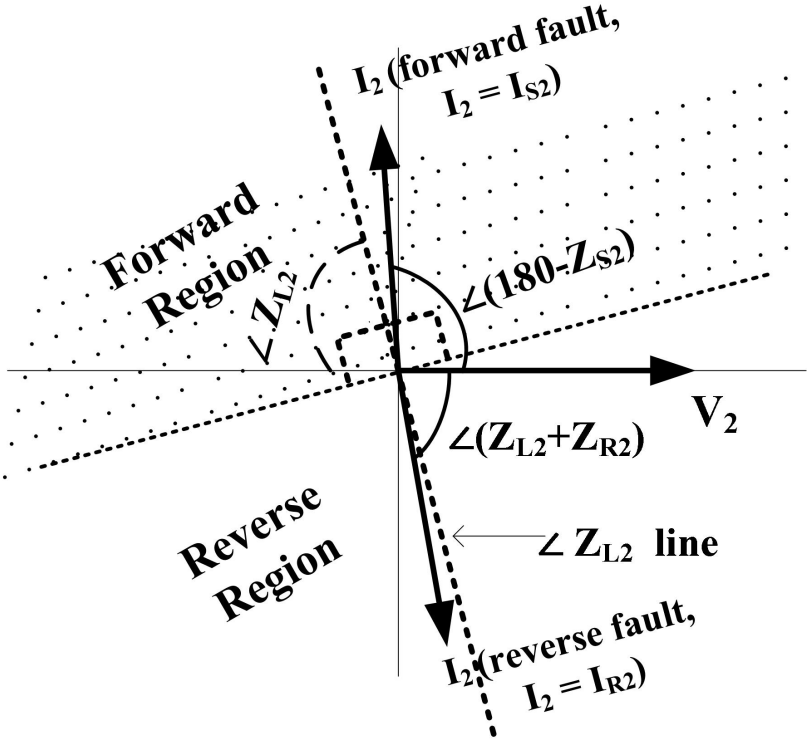

Figure 3.3: V_2 and I_2 phasors for Forward and Reverse Faults

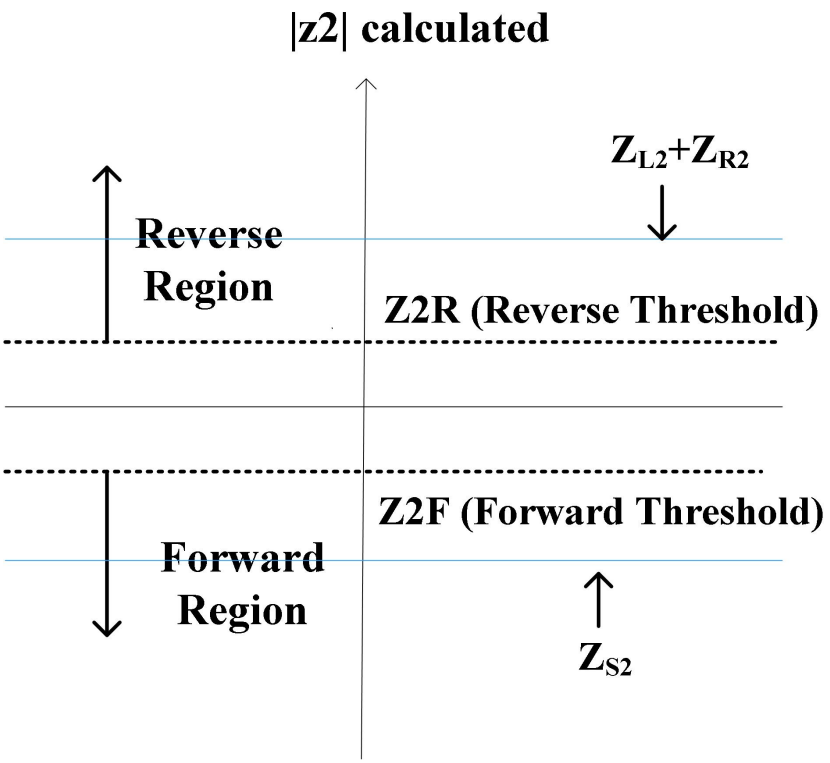

Figure 3.4: z_2 Magnitude and Thresholds for Forward and Reverse Faults [32]

Fig. 3.4 shows the z_2 magnitude calculated by the relay (3.7) based on the measured V_2 and I_2 values for forward and reverse faults. The figure also shows forward and reverse threshold impedance values set to the directional element. The directional element provides fault direction by comparing the calculated impedance value with threshold impedance values.

I_2 phasor position and the angle limits for forward and reverse faults are shown in Fig. 3.3. 90^0 either side of the $\angle Z_{L2}$ line forms forward region (top side) and other 180^0 forms reverse region. This way, the directional element segregates the fault direction based on the I_2 phasor position.

Negative-sequence directional element philosophy is developed based on traditional source negative-sequence current behavior, as we discussed above. If this directional element is to protect a Type-IV WPP, negative-sequence current from the WPP during fault conditions should be similar to a traditional source. This way

performance of the directional element for Type-IV WPP can be maintained.

3.3 Type-IV WTG Short Circuit Behavior

Type-IV WTGs are connected to the grid through inverters, and fast controls associated with the inverters define the short-circuit currents within the first few cycles of fault initiation. Unlike traditional sources, fault currents from these IBRs are injected into the grid as per the FRT conditions defined in the control system. I_2 phasor during unbalanced fault conditions is solely based on the inverter control system. This section discusses some of the Type-IV WPP inverter controls and their influence on the I_2 phasor.

Current controlled voltage source inverters are predominant in the present high megawatt-scale WPPs. These inverters use current controls in the inner loops, which are fast in nature. FRT conditions directly generate current references bypassing outer loop slow controls; hence defined fault behavior can be observed within the first 1 or 2 cycles. Grid codes cannot cover the entire control system; hence manufacturer-specific control objectives are also added to the FRT in addition to the grid codes. In addition to these current controls and FRT conditions, PLL also contributes to Type-IV WTG short circuit behavior. PLL plays a crucial role in sending the active and reactive power from IBR during normal and fault conditions as per the grid standards in synchronization with the grid [9]. Fault conditions associate with sudden phase angle jump, and unbalanced faults offer negative-sequence voltages. PLL should address these issues quickly and accurately. Inaccurate positive-sequence phase angle estimation could lead to unexpected negative-sequence currents.

The inverter control system classifies the current references into active currents and reactive currents, which are to be injected into the grid from the inverter. Control objectives or FRT is converted to these current references by using the mathematical equations for active power and reactive power in dq-frame [13].

Broadly, inverter current controls can be classified into coupled-sequence current control (or coupled control) and decoupled sequence current control.

- Coupled Control (CC):

  CC generates references I_d and I_q based on the positive-sequence active and reactive power requirements. Against these references, feedback current and voltage signals from the measuring point are compared, and error signals are generated to take the corrective action. Here, the feedback signals are not completely free from negative-sequence quantities (unlike decoupled-sequence control). Because of this reason, IBR injects some negative-sequence currents. Negative-sequence currents can also be possible due to other reasons like phase shift in the measurement systems [19]. CC does not have any control objective for negative-sequence currents; hence there can be some small amount of negative-sequence currents that are generated as mentioned above.

- Decouple Sequence Control (DSC)-1:

  Negative-sequence voltage present during unbalanced fault conditions or unbalanced load conditions can cause double-frequency oscillations in the inverter active power. By having certain magnitude and phase angle of the negative-sequence currents, these double-frequency oscillations can be eliminated. Double-frequency oscillations in the active power cause inverter DC input voltage fluctuations and disturb the maximum power point control (based on the DC voltage control) and also poses increased costs associated with the DC capacitor.

  IBR with the DSC-1 control generates positive-sequence as well as negative-sequence rotating frame I_d and I_q references, and feedback current and voltage signals used are properly decoupled from each other. This control generates positive-sequence I_d and I_q (active and reactive) references just like in CC.

Negative-sequence I_d and I_q (active and reactive) references are calculated based on the control objective to mitigate the double-frequency oscillations in the inverter active power [19].

- Decouple Sequence Control (DSC)-2:

  This control regulates the positive as well as negative-sequence currents as per the FRT conditions mentioned in the German grid code. Negative-sequence I_d and I_q (I_2-active and I_2-reactive) references are generated by solving the P_2 and Q_2 equations to achieve the German grid code requirements.

3.4 Traditional Sources vs German Grid Code-Based Type-IV WPP Negative-Sequence Components Behavior during Faults

Recent German grid code (VDE-AR-N 4120) mentioned in [31], [19] seems to be more practical way (under its inverter current limits) of IBR control system which can have a negative-sequence fault behavior like a conventional source.

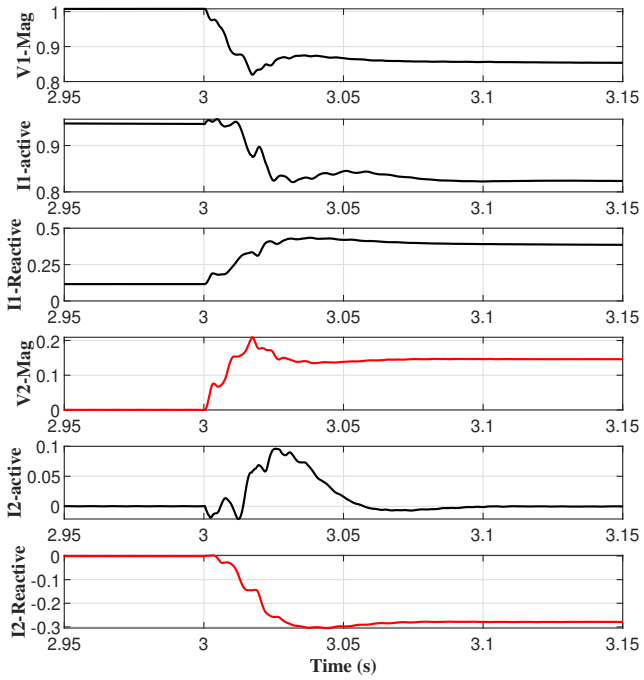

Figure 3.5: German Grid Code-based WPP Fault Behavior

Conventional source I_2 phasor is based on the negative-sequence network diagram R and X_L components from the fault point to the source. The fault point being the maximum unbalance point acts like a negative-sequence voltage source. Conventional source consumes negative-sequence active power(P_2) and negative-sequence reactive power (Q_2). P_2 and Q_2 are proportional to R and X_L of the negative-sequence network from the fault point to the source, respectively. However, Type-IV WPP P_2 and Q_2 are based on the inverter control system and FRT conditions. Type-IV WPP with a German grid code-based control system have Q_2 (I_2-reactive) just like a conventional source. P_2 (I_2-active) is not defined in the grid code so that P_2 changes based on the control objectives defined to the control system. For this thesis work, DSC-2 control developed by selecting P_2 as zero as part of FRT conditions. Hence, irrespective of the system R and X_L, this control have I_2 phasor perpendicular to V_2 during unbalanced fault conditions. This type of fault behavior can be observed in conventional sources with highly inductive dominant systems.

For a forward fault, Type-IV WPP with DSC-2 control I_2 leads V_2 by 90^0. This fault behavior is in line with conventional sources. Due to this fact, Negative-sequence directional element which is developed based on the conventional sources fault behavior, can very well be applied with Type-IV WPPs with this DSC-2 control.

3.5 Proposed Modification

German grid code-based control system negative-sequence fault behavior is in line with the traditional sources. The negative-sequence directional element can be applied to German grid code-based control implemented Type-IV WPP. However, the German grid code is not solving the problem completely. Unlike traditional sources with high magnitudes of fault currents, IBR fault currents are restricted to rated currents. German grid code-based control sees only V_2 at the inverter terminal and injects negative-sequence current magnitude (I_2) proportional to a number 'k'. For high impedance faults, V_2 at the inverter terminals will be low; hence I_2 also will have a

small magnitude. As discussed in section 2.2, there is a relay setting that ensures I_2 to be minimum a2 times of I_1 for the negative-sequence directional element to give a directional decision. This setting a2 for the German grid code control based Type-IV WPP is not satisfied for some of the high impedance fault case scenarios (when k value taken as 2), especially during high pre-fault power conditions. High value of I_1 is the reason for $\frac{|I_2|}{|I_1|}$ ratio to go below a2 setting.

Proposed modification to the directional element logic:

- Directional element logic may be modified by changing $\frac{|I_2|}{|I_1|}$ (a2 setting) to $\frac{|I_2 - reactive|}{|I_1 - reactive|}$, making the directional element a2 setting independent of the I_1-active current component. This can improve the dependability of the negative-sequence directional element.

CHAPTER 4: TEST SYSTEM, RESULTS, ANALYSIS AND RECOMMENDATIONS

4.1 Overview

In this chapter, the test system developed in EMTP-RV is explained first. The test system description includes the current reference generation for the three Type-IV WPP control models. Then, MATLAB developed (software) negative-sequence directional element settings are presented. Later, various unbalanced fault cases are presented. Then, AG fault results are presented for conventional source and German grid code-based model. Then, results are presented for the directional element with proposed a2 factor modification. Later, all results are analyzed, and then recommendations are provided for improving the performance of the directional element for Type-IV WPP.

4.2 Test System

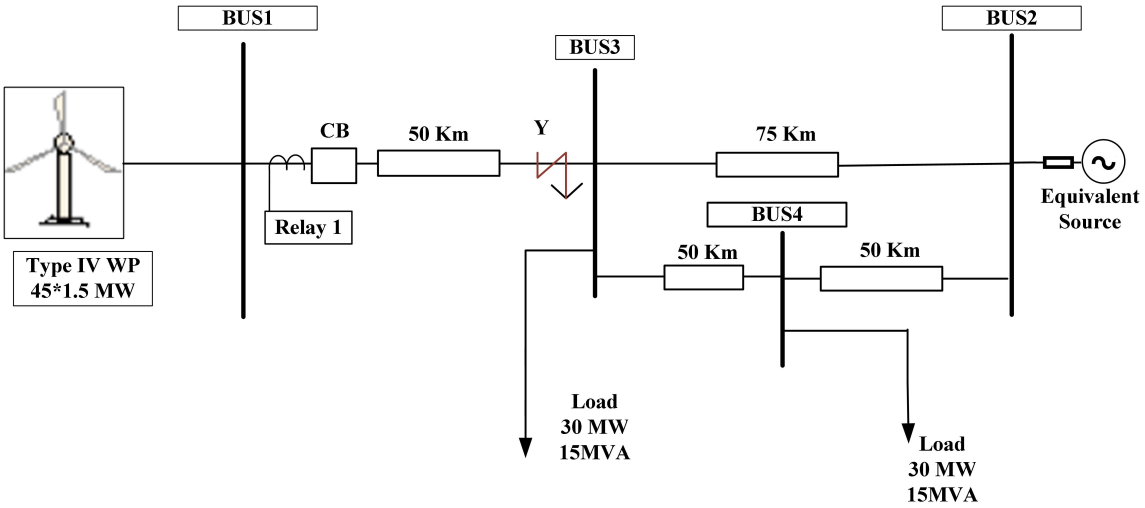

Figure 4.1: Test System Single Line Diagram

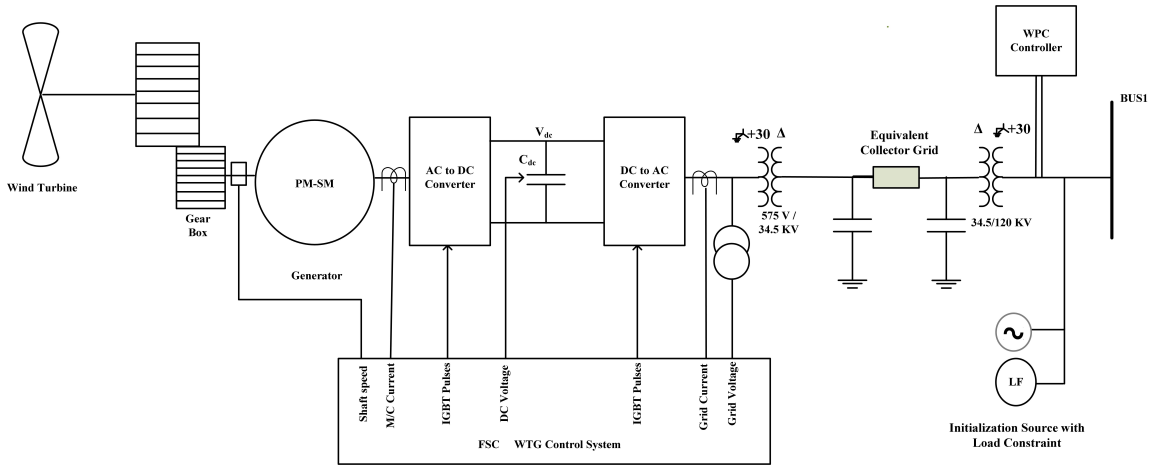

Figure 4.2: WPP Single Line Diagram

Fig. 4.1 shows the WPP connection to the traditional source via a transmission line. Relay1 is placed at bus1. Fault cases are applied at the location 'Y', which is at 100% of the transmission line-13. Fig. 4.2 shows the Type-IV WPP single line diagram. The collector grid is represented as equivalent π (assumption). At the inverter terminals, all measurements are sent to the inverter control system. The figure also shows two transformers to step-up the voltage to transmission level, i.e., from 575V to 120KV.

4.2.1 WPP Model with Coupled Control (CC)

Coupled control mode of operation generates only positive-sequence d-axis and q-axis current references required by the current controlled VSI, and this control does not have any negative-sequence current references.

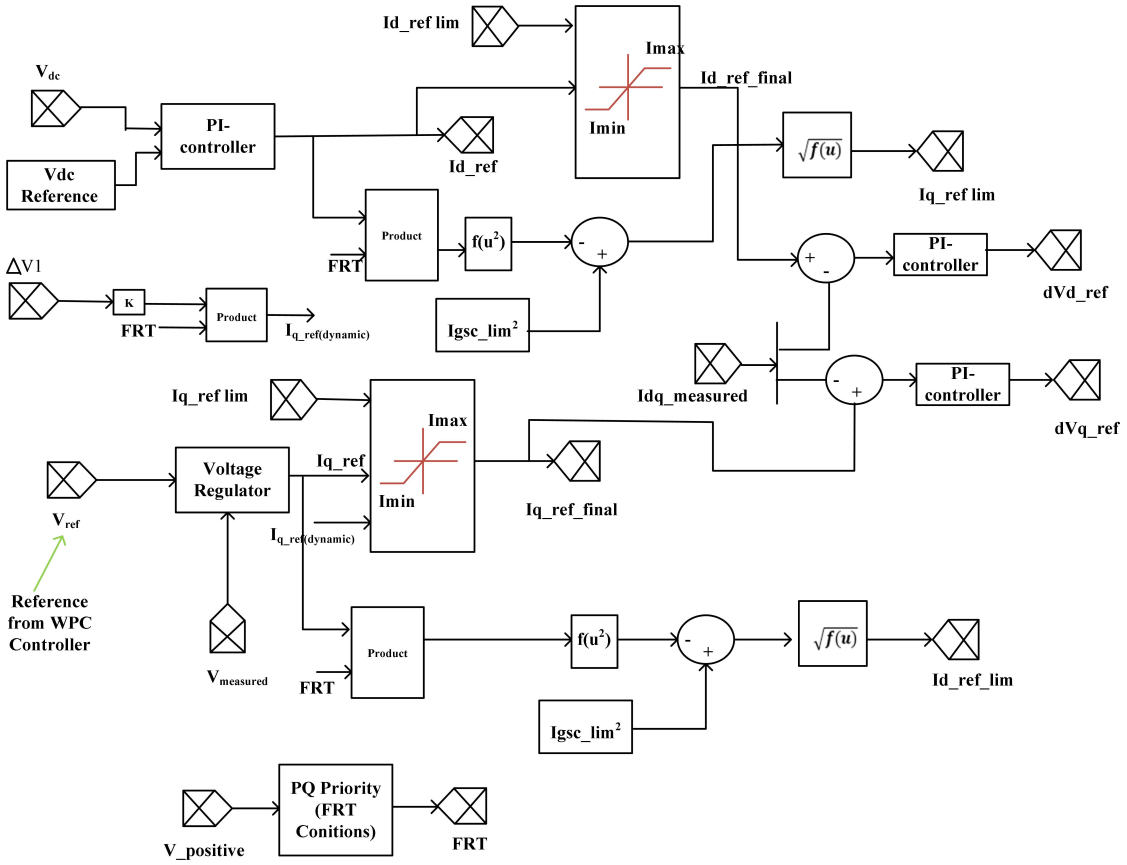

Figure 4.3: Coupled Control

Fig. 4.3 shows the current reference generation for positive and negative-sequence currents. The figure also shows the application of limits during normal and FRT conditions.

For the positive-sequence system, The active power and reactive power equations [33] are as presented in equations (4.1) and (4.2) below,

$$P = \frac{1}{2}(v_d.i_d + v_q.i_q) \tag{4.1}$$

$$Q = \frac{1}{2}(v_q.i_d - v_d.i_q) \tag{4.2}$$

Phase-locked loop (PLL) as we discussed in section 2.4.2 estimates phase angle θ by tracking v_q to zero. Hence, active power depends only on i_d and reactive power

depends only on i_q.

d-axis current reference:

This component of the current decides the active power from the inverter. DC voltage value varies based on the mismatch between the input power supplied by the wind turbine and inverter output power. If the wind turbine sends more or less power to the DC system compared to the active power sent out from the inverter, DC system voltage increases or reduces, respectively. To maintain the steady-state DC Voltage with varying weather conditions, PI controller generates the d-axis current reference for the inverter by looking at the DC voltage.

q-axis Current reference:

This component of current decides the amount of reactive power supplied by the inverter. i_q reference depends on FRT conditions and selection of control such as Q-control or pf control or V-control.

During FRT conditions dynamic reactive current that is needed to sent by the WPP is provided to the control system by the equation (4.3),

$$i_{qref} = k * (V_{ref} - V_{wt}^{+}) \tag{4.3}$$

k - multiplication factor defined by the transmission system operator (TSO)

V_{wt}^{+} - positive-sequence voltage at the inverter's terminal

V_{ref} - generally set to 1 p.u.

PQ Priority:

During normal operating conditions, i_{dref} (active power P) have the priority and i_{qref} is restricted accordingly to keep the inverter current within limits. This iq reference current limit is calculated, as shown in equation (4.4).

$$i_{qref-lim} = \sqrt{(i_{lim}^2 - i_{dref}^2)} \tag{4.4}$$

During FRT condition, i_{qref} (reactive power) have the priority and i_{dref} is restricted accordingly to keep the inverter current within limits. This id reference current limit is calculated, as shown in equation (4.5).

$$i_{dref-lim} = \sqrt{(i_{lim}^2 - i_{qref}^2)} \tag{4.5}$$

This concludes, out of total current limit set for the inverter (i_{lim}), the current component with high priority gets fulfilled wholly based on the system operating conditions, and then the other component is adjusted or limited.

4.2.2 WPP Model with Decoupled Sequence Control-1

DSC-1 control implemented Type-III WPP fault response is validated with field relay recordings [34] . Majorly, this control model differs with others, by calculating negative-sequence components to make the active power free from double-frequency oscillations. This model uses eight measurements v_d^+, v_q^+, v_d^-, v_q^-, i_d^+, i_q^+, i_d^- and i_q^- and generates 4 output current references i_d^{+*}, i_q^{+*}, i_d^{-*} and i_q^{-*}.

DSC-1 control generates negative-sequence and positive-sequence current references based on the following matrix equation (4.8). Positive-sequence i_q reference first calculated based on the k-factor just like in CC, then remaining current references are generated as follows.

$$P = P_0 + P_{c2}\, cos(2wt) + P_{s2}\, sin(2wt) \tag{4.6}$$

$$Q = Q_0 + Q_{c2}\, cos(2wt) + Q_{s2}\, sin(2wt) \tag{4.7}$$

Double-frequency oscillations in active power and reactive power are as shown in

equations [35] (4.6) and (4.7).

$$\begin{bmatrix} i_q^{+*} \\ i_d^{+*} \\ i_q^{-*} \\ i_d^{-*} \end{bmatrix} = \begin{bmatrix} 1 & 0 & 0 & 0 \\ v_q^+ & v_d^+ & v_q^- & v_d^- \\ v_q^- & v_d^- & v_q^+ & v_d^+ \\ -v_d^- & v_q^- & v_d^+ & -v_q^+ \end{bmatrix} + \begin{bmatrix} i_{qref} \\ P_0 \\ P_{C2} \\ P_{S2} \end{bmatrix} \tag{4.8}$$

Matrix equation 4.8 provides current references to bring down P_{C2} and P_{S2} to zero.

PQ priority is just like in coupled control, during normal operating conditions, P or i_d reference have the priority i.e. i_d is utilized till the inverter limits and i_q is restricted as in (4.9).

$$i_{qref-lim} = \sqrt{(i_{lim}^2 - i_{dref}^2)} \tag{4.9}$$

During FRT conditions, Q or i_q reference have the priority i.e. i_q is utilized till the inverter limits and i_d are restricted as in (4.10).

$$i_{dref-lim} = \sqrt{(i_{lim}^2 - i_{qref}^2)} \tag{4.10}$$

Current limits for i_{dref} and i_{qref} are just like in CC control. However, for this DSC-1 control there is another level of current limits i.e. sequence components shares the limits as shown in equations (4.11) and (4.12) ,

$$i_d^{+*} + i_d^{-*} <= i_{dlim} \tag{4.11}$$

$$i_q^{+*} + i_q^{-*} <= i_{qlim} \tag{4.12}$$

If the current references cross their respective limiting conditions, new references are generated as shown in equations (4.13), (4.14), (4.15) and (4.16),

$$i_{dnew}^{+*} = i_d^{+*} . \frac{i_{dlim}}{(i_d^{+*} + i_d^{-*})} \tag{4.13}$$

$$i_{dnew}^{-*} = i_d^{-*} . \frac{i_{dlim}}{(i_d^{+*} + i_d^{-*})} \tag{4.14}$$

$$i_{qnew}^{+*} = i_q^{+*} . \frac{i_{qlim}}{(i_q^{+*} + i_q^{-*})} \tag{4.15}$$

$$i_{qnew}^{-*} = i_q^{-*} . \frac{i_{qlim}}{(i_q^{+*} + i_q^{-*})} \tag{4.16}$$

These limiting conditions are important as the inverter output currents gets altered from the FRT when the FRT generated references are more than the current limits.

4.2.3 WPP Model with Decoupled Sequence Control-2

This control regulates the positive as well as negative-sequence currents as per the FRT conditions mentioned in the German grid code. Positive-sequence d and q current references are just as presented in WPP with CC control. Negative-sequence current references are as shown in equations below,

$$i_{qref^-} = k * V_{wt}^- \tag{4.17}$$

$$i_d^{-*} = i_{qref^-} * \frac{-v_q^-}{(v_d^-)^2 + (v_q^-)^2} \tag{4.18}$$

$$i_q^{-*} = i_{qref^-} * \frac{v_d^-}{(v_d^-)^2 + (v_q^-)^2} \tag{4.19}$$

Unlike positive-sequence q reference voltage v_q^+ which is tracked to zero by PLL, negative-sequence q reference voltage v_q^- is not tracked to zero. Hence negative-sequence active power depends on d-axis as well as q-axis current references (refer equations (4.1) and (4.2)). Negative-sequence reactive power also depends on d-axis as well as q-axis current references. Whereas positive-sequence active power is dependent on d-axis current only, and reactive power is dependent on q-axis current only. For this DSC-2 control, $P_2 = 0$ and $Q_2 = k * V_{wt}^-$ are achieved using the equations (4.17), (4.18) and (4.19).

Current limits for these four current references i_d^{+*}, i_q^{+*}, i_d^{-*} and i_q^{-*} are calculated

just like in DSC-1 control.

4.2.4 Conventional Source Model

EMTP-RV test system Type-IV WTG (upto inverter) is replaced with a conventional source keeping the remaining system as it is. Conventional source is connected to the collector grid as shown in Fig. 4.1. Conventional source impedance ratio (SIR) is selected to 165% of the transmission line to match the fault current for LLL fault applied at Bus-1 with that of Type-IV WPP. This test system is used for comparing the fault behavior of Type-IV WPP.

4.3 Negative-Sequence Directional Element (Software) Settings

Fault data collected in the form of COMTRADE files are read from MATLAB and then MATLAB developed directional element is used to observe the directional decision.

Table 4.1: Directional Element Settings

Setting Name	Setting value
Z2F	-0.3 ohms
Z2R	0.3 ohms
50FP (3*I_2)	0.3 A
50RP (3*I_2)	0.3 A
a2 ($\|I_2\|/\|I_1\|$)	0.2
k2 ($\|I_2\|/\|I_0\|$)	0.2
ECA	75.16^0

This directional element calculates the negative-sequence impedance using equation (2.7) at the relay point shown in Fig. 4.1. Then settings shown in Table 4.1 are applied to provide the fault direction.

4.4 Test Results for WPP with CC, DSC-1 and DSC-2 Controls

Table 4.2: Directional Element Results for Rf=0 and 1 p.u Pre-fault Power

Fault Location	Fault Type	Conventional Source	WPP Control		
			CC	DSC-1	DSC-2
Y	AG	32QF	N.O.	32QF	32QF
	BC	32QF	N.O.	32QF	32QF
	BCG	32QF	N.O.	32QF	32QF

Table 4.3: Directional Element Results for Rf=40 and 1 p.u Pre-fault Power

Fault Location	Fault Type	Conventional Source	WPP Control		
			CC	DSC-1	DSC-2
Y	AG	32QF	N.O.	N.O.	N.O.
	BC	32QF	N.O.	N.O.	32QF
	BCG	32QF	N.O.	N.O.	32QF

Table 4.4: Directional Element Results for Rf=40 and 0.5 p.u Pre-fault Power

Fault Location	Fault Type	Conventional Source	WPP Control		
			CC	DSC-1	DSC-2
Y	AG	32QF	N.O.	N.O.	32QF
	BC	32QF	N.O.	N.O.	32QF
	BCG	32QF	N.O.	N.O.	32QF

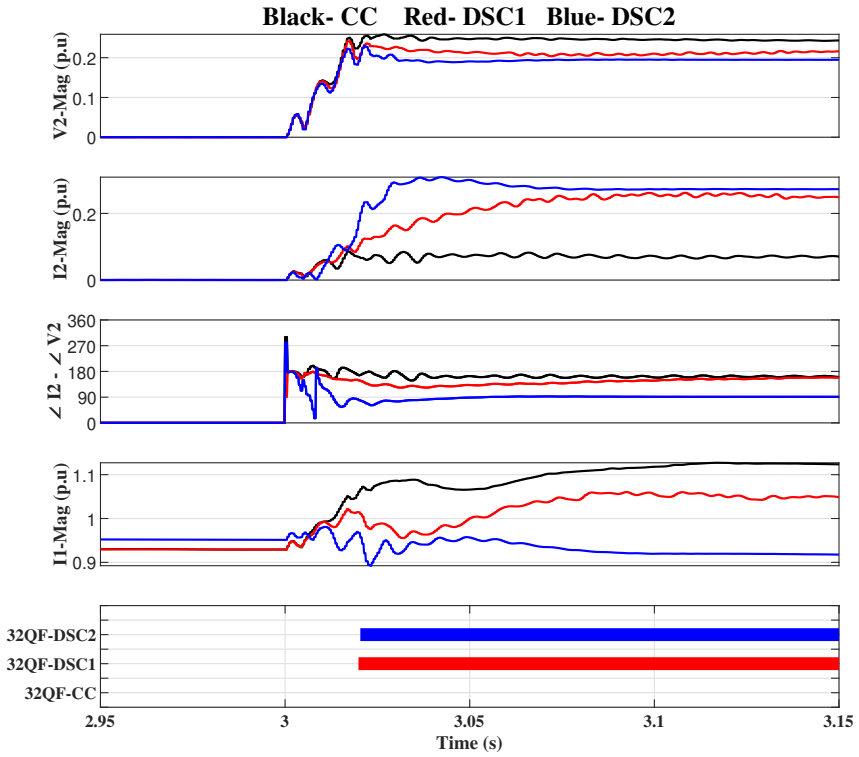

Figure 4.4: AG Fault Results at Bus1 with Rf=0 ohms and 1 p.u Pre-fault Power for Three WPP Controls

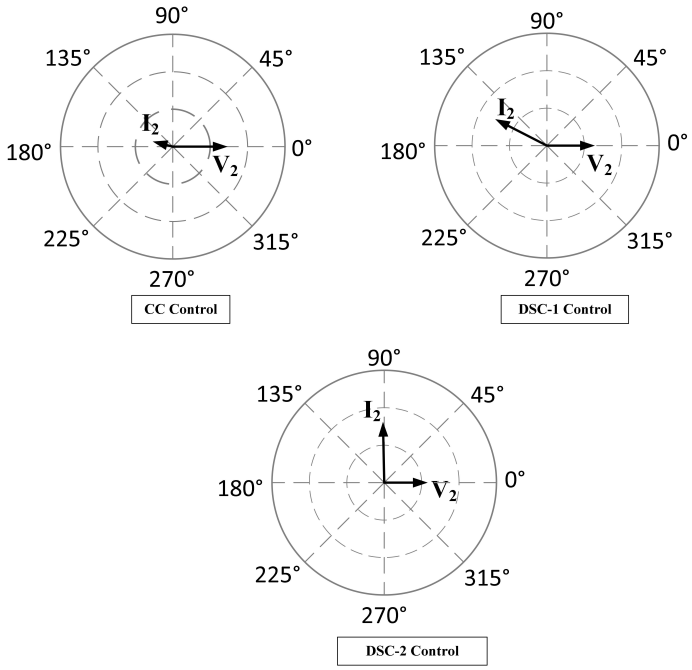

Figure 4.5: V_2 and I_2 Phasors for AG Fault for Rf=0 ohms and 1 p.u Pre-fault Power

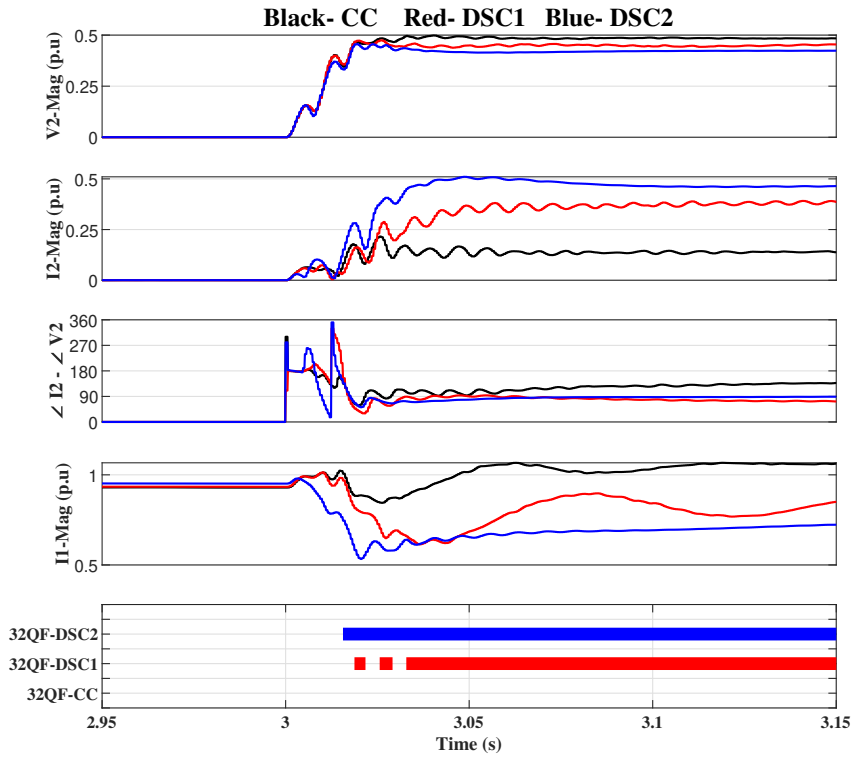

Figure 4.6: BC Fault Results for Rf=0 ohms and 1 p.u Pre-fault Power for the Three WPP Controls

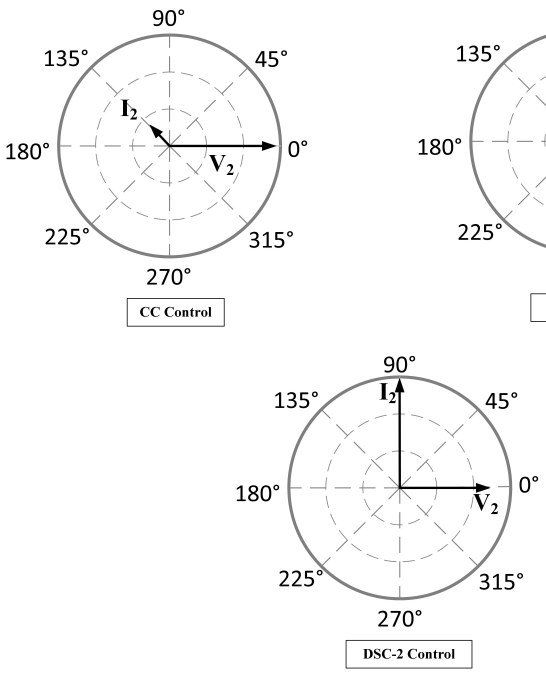

Figure 4.7: V_2 and I_2 Phasors for BC Fault for Rf=0 ohms and 1 p.u Pre-fault Power

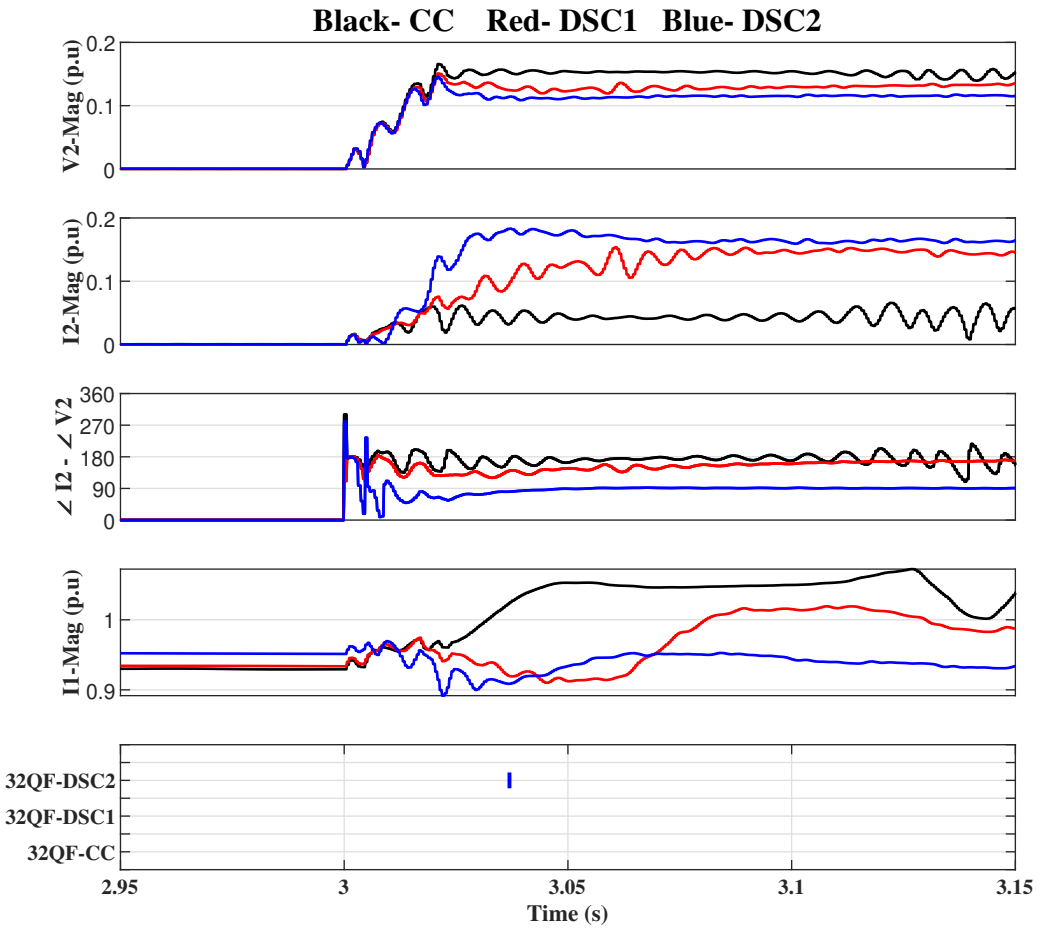

Figure 4.8: AG Fault Results for Rf=40 ohms and 1 p.u Pre-fault Power

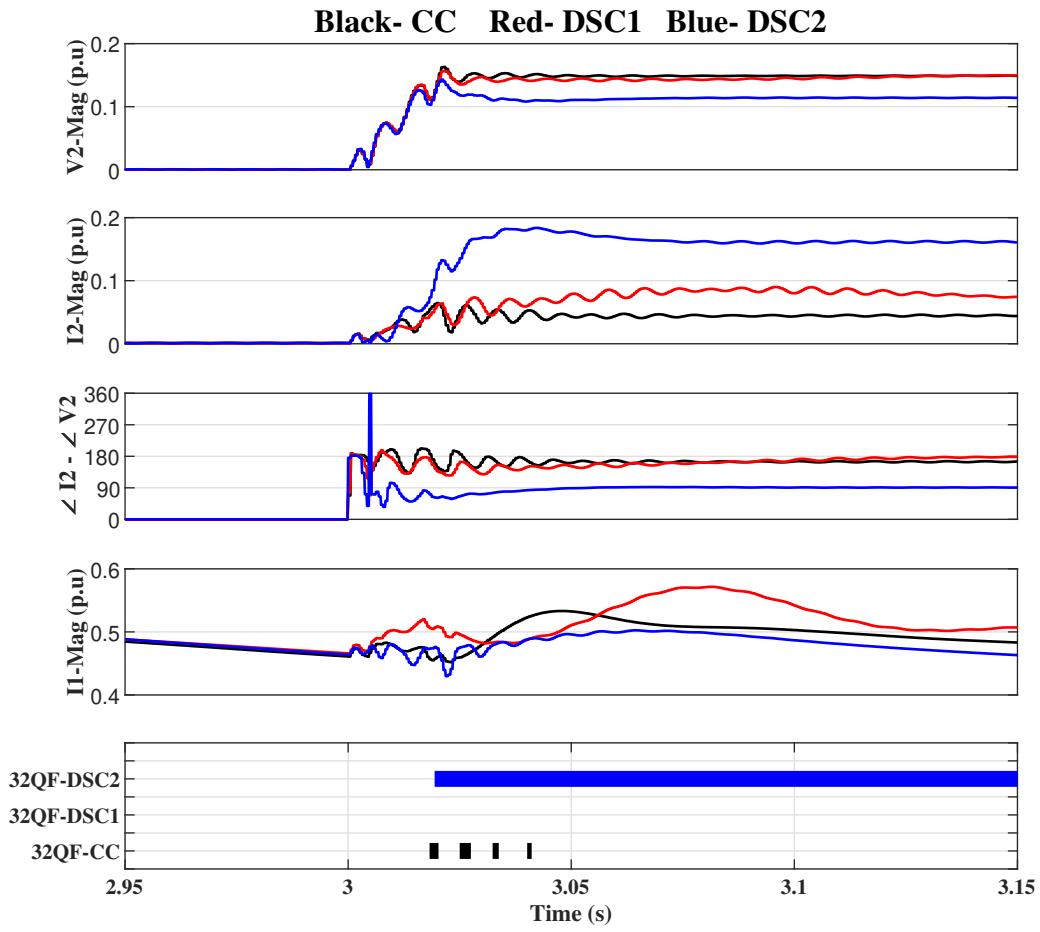

Figure 4.9: AG Fault Results for Rf=40 ohms and 0.5 p.u Pre-fault Power

4.5 Test Results for the Conventional Source and WPP with DSC-2 Control

In this section, conventional source AG fault results and German grid code based Type-IV WPP model results are presented.

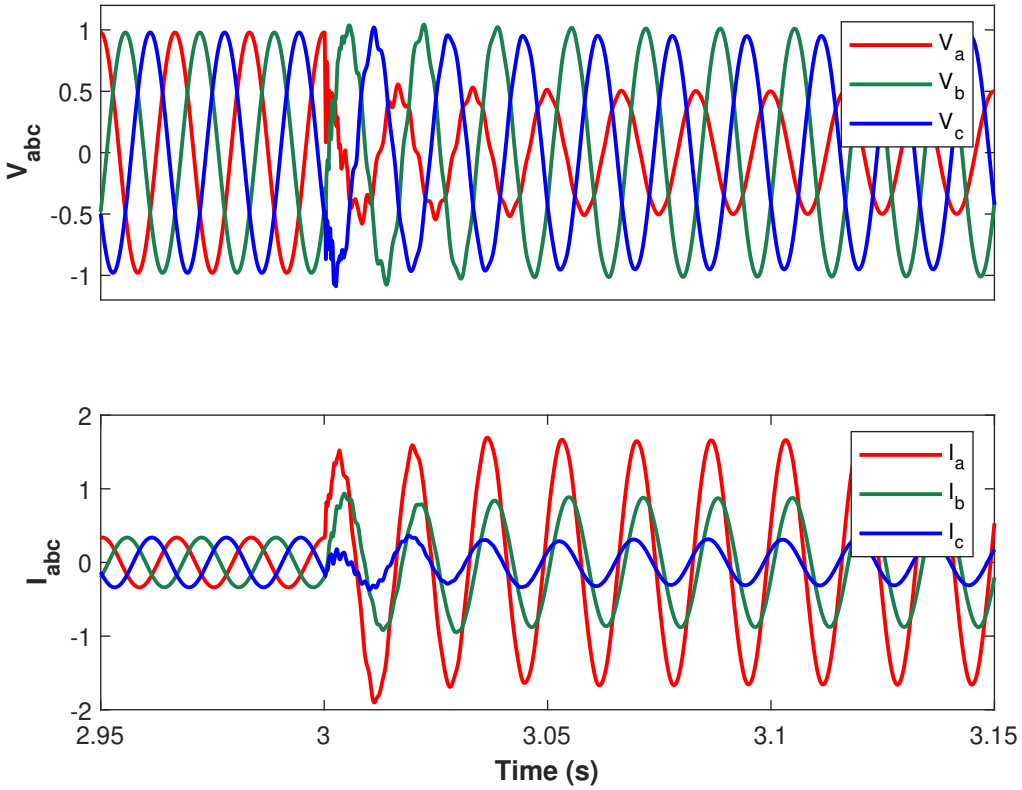

Figure 4.10: AG fault Vabc, Iabc results for Rf=0 ohms for Conventional Source at Relay1

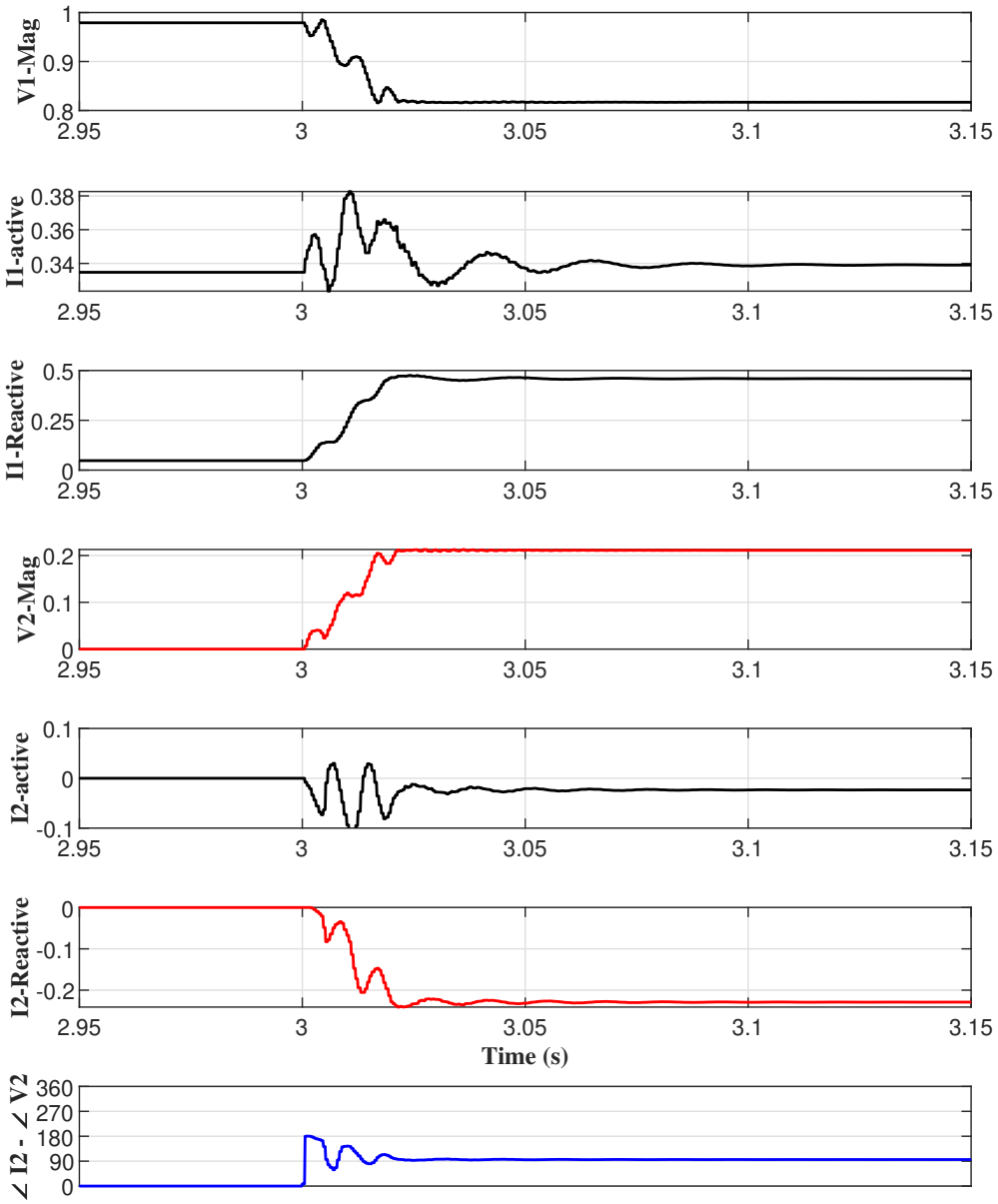

Figure 4.11: AG Fault Sequence Components Results for Rf=0 ohms for Conventional Source at Relay1

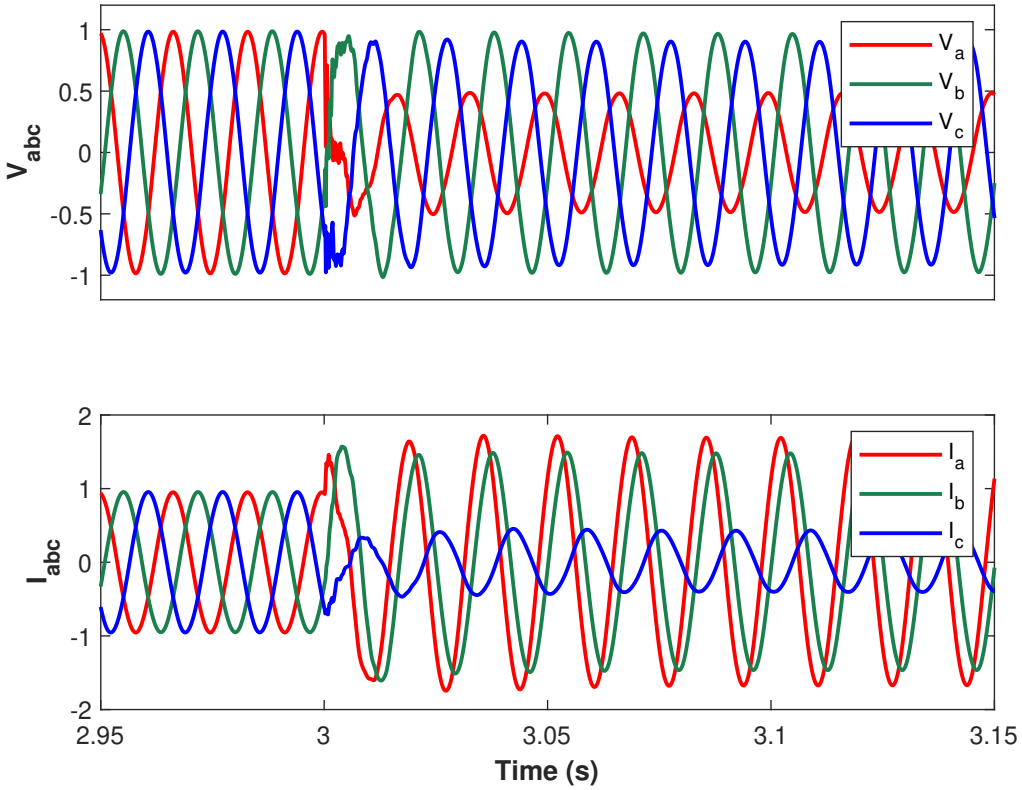

Figure 4.12: AG Fault Vabc, Iabc Results for Rf=0 ohms for German Grid Code-based WPP at Relay1

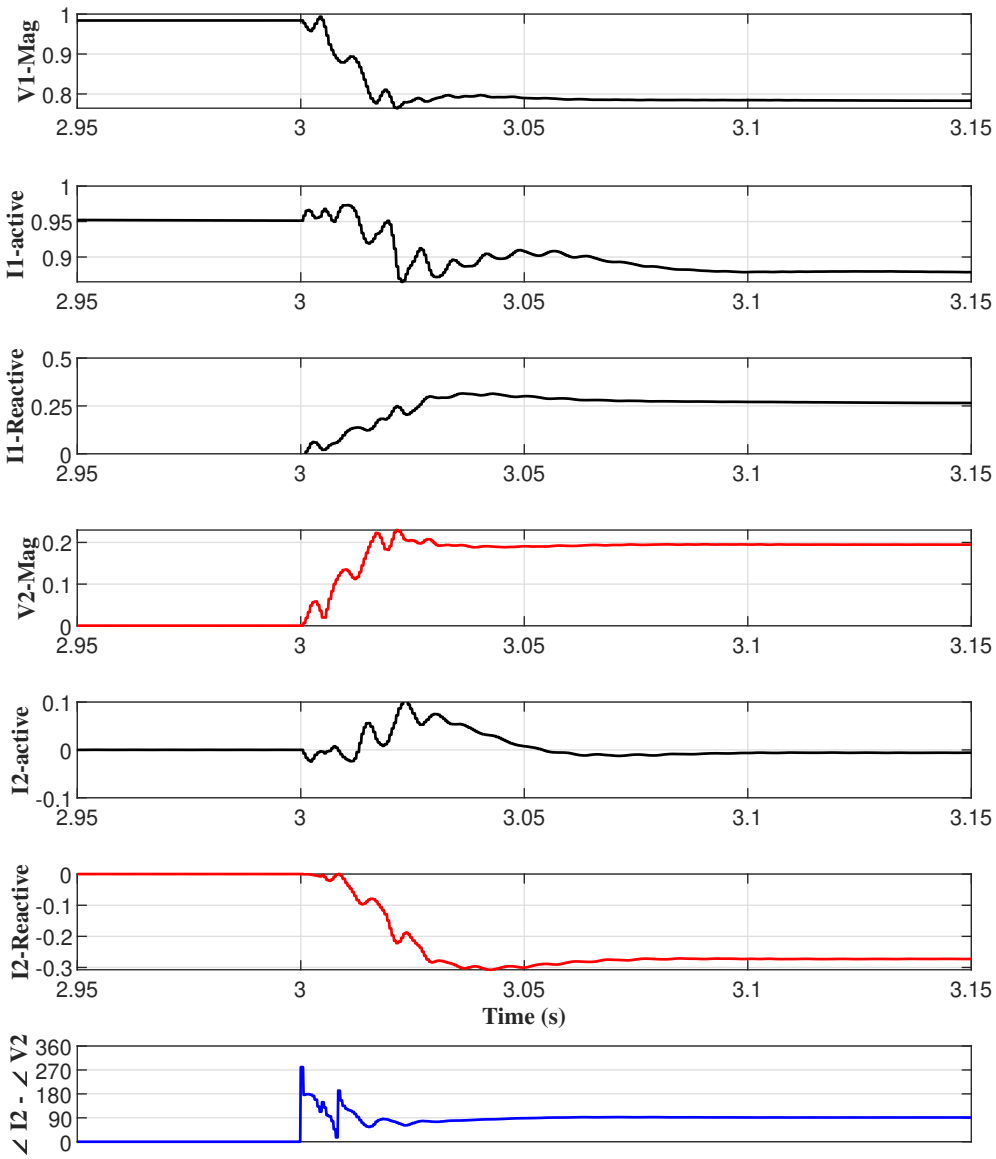

Figure 4.13: AG Fault Sequence Components Results for Rf=0 ohms for German Grid Code-based WPP at Relay1

4.6 Analysis of Fault Results

Tables 4.2, 4.3 and 4.4 show the directional decision by the directional element for faults AG, BC, BCG for three cases (fault resistance 0 ohms with 1 p.u pre-fault power, 40 ohms with 1 p.u pre-fault power and 40 ohms with 0.5 p.u pre-fault power). These directional element results reveal WPP with CC control caused no directional decision for all the fault cases. WPP with DSC-1 control resulted in the proper direction for only Rf=0 ohms case. DSC-2 control resulted in the proper directional decision for all the cases except for one case, i.e., AG fault with 40 ohms and 1 p.u pre-fault power.

Analysis of fault results for CC control

WPPs with CC control when feeding faults, FRT conditions make the Q priority over P, this shift caused to increase in I_1-reactive and decrease in I_1-active keeping overall current magnitude within inverter current limit 1.1 p.u. From the Fig. 4.4, and Fig. 4.6, WPP, which was operating I_1 at 1 p.u before applying the fault, raised to 1.1 p.u after applying the fault. Here change in I_1 magnitude is minimal, but there is a remarkable change in positive-sequence phase angle (not shown in the figures plotted as this phase angle change has no importance for negative-sequence directional element). CC control does not specify any negative-sequence currents that are to be injected into the grid during FRT. Though there is a small amount of I_2 (as mentioned in section 3.3), its magnitude is observed to be increasing with the magnitude of V_2 (Fig. 4.4 and Fig. 4.6). Negative-sequence phase angle is also varying from fault to fault. Minimum I_2 (50 FP/50 RP, a2, and k2) interlocks have inhibited the directional decision, for both AG fault (Fig. 4.5) and for BC fault (Fig. 4.7). WPPs with CC control poses both dependability and security issues to the directional element.

Analysis of fault results for DSC-1 control

WPPs with DSC-1 control when feeding faults, positive-sequence currents behave the same as the CC control. DSC-1 control has a particular objective to inject negative-sequence currents during FRT, as discussed in section 4.2.2. Two things again, I_2-magnitude and negative-sequence phase angle, which are of interest for directional element. Though I_2 magnitude is higher for this control model than CC control, I_2 phasor (I_2 magnitude and I_2 phase angle with respect to V_2 phase angle) depends on the V_2 phasor. It is observed from AG and BC fault results, I_2 magnitude is increased with V_2, and I_2 phase angle is not the same for both cases. Negative-sequence phase angle is varying from fault to fault (Fig. 4.5 and Fig. 4.7). This change in phase angle observed to be within the forward direction angle limits, i.e., from 14.84^0 to 194.84^0 for set ECA=75.16^0. WPP with DSC-1 control resulted in the proper operation of traditional negative-sequence directional element for all three unbalanced faults applied with Rf=0 ohms (table 4.2). Nevertheless, the magnitude of I_2 is low compared to DSC-2 and traditional systems fault cases, and the negative-sequence phase angle is inconsistent. As I_2 is dependent on V_2-magnitude, negative-sequence directional element dependability issues observed for high impedance faults (Fig. 4.8 and Fig. 4.9), where V_2-magnitude at the inverter terminal is low (4.3 and 4.4).

Analysis of fault results for DSC-2 control

WPPs with DSC-2 control when feeding the faults are shown to have a similar negative-sequence current behavior like a reactive (inductive) dominant traditional system (including sources and lines, cables, etc.), except the fact that the current magnitude is comparatively low. However, I_2-magnitude is higher compared to CC-control and DSC-1 control. The negative-sequence phase angle is close to 90^0 leading for all the forward unbalanced faults (Fig. 4.5 and Fig. 4.7). Negative-sequence

directional element is operated for all the three faults with Rf=0 ohms (table 4.2). As discussed in section 4.2.3, I_2 magnitude is k-times of V_2 magnitude (V_2 measured at the inverter terminals). For high impedance faults (Fig. 4.8 and Fig. 4.9) I_2-magnitude injected to the grid is small (0.16 p.u for both cases). The reason for this low I_2 value is due to V_2 at the inverter terminals is low (fault point V_2 itself low due to less unbalance with high fault impedance). Here, for the same amount of I_2-magnitude, one case resulted in the proper directional decision and another case with in no directional decision. No directional decision happened due to a2 setting in the relay logic. During rated operating conditions, I_1-active is high and inhibited directional decision. German grid code implemented WPP if sending low I_2 current (even with the consistent negative-sequence phase angle), it may not be sufficient to satisfy minimum I_2 current requirements mentioned for the directional element, and so can pose dependability issues for the directional element.

Type-IV WPPs with DSC-2 control offered more negative-sequence currents than other two controls, hence, V_2 magnitude for DSC-2 is observed to be lower for the same fault case compared to CC-control and DSC-1 control (this is one reason for the German grid code specifying the negative-sequence current requirement). Positive-sequence current is observed to be low for DSC-2 control (Fig. 4.4 and Fig. 4.6) compared to other two controls (I_1-active got reduced with the increase in I_2 current), as the inverter current limiters are restricting the total current (summation of I_1 and I_2) flowing out from the inverter.

Analysis of results for traditional source vs German grid code based Type-IV WPP

Traditional source negative-sequence phase angle and German grid code based Type-IV WPP negative-sequence phase angle, are the first to observe. For the both cases, negative-sequence phase angle ($\angle I_2$-$\angle V_2$) is close to 90^0 leading (Fig. 4.11 and Fig. 4.13). I_2-active is little higher for traditional sources but not significant when compared to I_2-reactive. Traditional source SIR is selected as a high value (weak

source) to match the ABC fault at Bus1 result with the Type-IV WTG model. Due to the high source reactance compared to the line, traditional source negative-sequence behavior is closer to pure inductive system, and the negative-sequence phase angle is close to 90^0. For strong sources, this phase angle will be little higher than 90^0 for a forward fault as I_2-active will be higher (proportional to R/X, refer 3.5). Fig. 4.10 and Fig. 4.12 reveals, phase voltages are similar for both cases (this is true for other WPP controls also), but the phase currents are not exactly the same. This deviation in currents can be attributed to zero-sequence currents which modifies the phase currents, and also due to mismatch in the negative-sequence current magnitudes. Nevertheless, negative-sequence currents magnitude and phase angle are very close and so negative-sequence directional element theory works well for German grid code based Type-IV WPP just as it works for traditional sources.

4.7 Directional Element Results after Implementing the Proposed Modification for Relay Logic

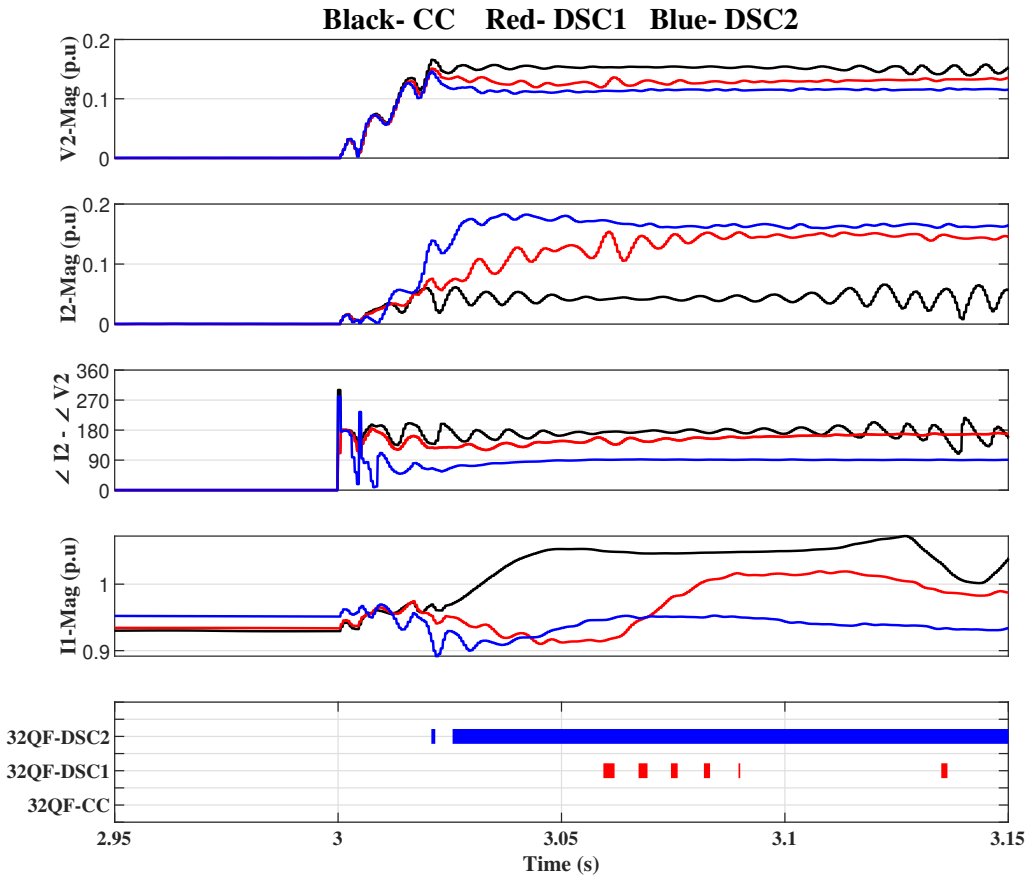

Figure 4.14: AG Fault Results for Rf=40 ohms and 1 p.u Pre-fault Power for Three Controls at Relay1 with Modified Logic

Table 4.5: Directional Element Results with Modified Relay Logic for Rf=0 and 1 p.u Pre-fault Power

Fault Location	Fault Type	Conventional Source	WPP Control		
			CC	DSC-1	DSC-2
Y	AG	32QF	N.O.	32QF	32QF
	BC	32QF	N.O.	32QF	32QF
	BCG	32QF	N.O.	32QF	32QF

Table 4.6: Directional Element Results with Modified Relay Logic for Rf=40 and 1 p.u Pre-fault Power

Fault Location	Fault Type	Conventional Source	WPP Control		
			CC	DSC-1	DSC-2
Y	AG	32QF	N.O.	N.O.	32QF
	BC	32QF	N.O.	N.O.	32QF
	BCG	32QF	N.O.	N.O.	32QF

Table 4.7: Directional Element Results with Modified Relay Logic for Rf=40 and 0.5 p.u Pre-fault Power

Fault Location	Fault Type	Conventional Source	WPP Control		
			CC	DSC-1	DSC-2
Y	AG	32QF	N.O.	N.O.	32QF
	BC	32QF	N.O.	N.O.	32QF
	BCG	32QF	N.O.	N.O.	32QF

Directional element rendered decision Fig. 4.14 for the DSC-2 control during high impedance and 1 p.u pre-fault power condition, which is the only case where directional element not operated (refer Fig. 4.8) with the original logic for DSC-2 control. Tables 4.5,4.6 and 4.7 shows the other fault cases directional element results with this

modified logic.

4.8 Recommendations

From the analysis, it is seen that the German grid code-based control system for a Type-IV WPP is recommended over other controls for the proper operation of the traditional directional element. In addition to the German-grid code controls, the following recommendations should also be taken into account to improve the dependability and security of the negative-sequence directional element.

- The inverter controls should have an extra feature to inject minimum $\frac{|I_2|}{|I_1|}$ by varying the k_{neg} (k multiplier for $|I_2|$) dynamically from 2 to 6 (minimum and maximum values for k), which can help overcome the dependability issues arising for high impedance faults.

- Alternatively, directional element logic may be modified by changing $\frac{|I_2|}{|I_1|}$ (a2 setting) to $\frac{|I_2-reactive|}{|I_1-reactive|}$. This change can make the directional element a2 setting independent of the active current component and improves the dependability of the negative-sequence directional element. Fault currents as well as the magnitude of negative-sequence currents are smaller for IBRs when compared to traditional sources, therefore relay logic should be judiciously used for these low values.

- The German grid code does not explicitly mention negative-sequence active current. If the IBR manufacturer uses I_2-active to define any control objective, it will cause the negative-sequence phase angle to shift from 90^0. If IBR injects I_2-active into the grid, instead of consuming it, the negative-sequence network R_2-source cannot be represented with a passive element and may cause directional element security issues when negative-sequence phase angle goes out of the forward directional angle limits. In order to address this, the inverter controls during FRT should follow I_2-active as zero or some negative value, such as I_2-

active=I_2-reactive*(R_2/X_2) (just as in the case of a system with a traditional source).

- Alternatively, the negative-sequence directional element can be slightly modified to make it independent of I_2-active by selecting ECA setting for the directional element as 90^0 instead of line impedance angle.

  Traditional sources negative-sequence phase angle depends on the source impedance angle and lines/cables impedance angle. However, for an IBR, the negative-sequence phase angle depends only on the FRT and independent of the line impedance. IBR control system can modify the $X_{2-source}$ and $R_{2-source}$ in such a way it always maintains the defined FRT negative-sequence currents to inject from the inverter. Hence, while setting the ECA for the directional element, instead of the line impedance angle, the control system FRT may be considered, which can make more sense.

  Traditional negative-sequence directional element theory depends on the magnitude of negative-sequence impedance-based, or we can also say, based on the negative-sequence apparent power flow direction (numerator of eq.3.7). For an IBR with the German grid code based control system (DSC-2), FRT defines the negative-sequence reactive current direction and not defines the negative-sequence active current. Hence, if ECA is set to 90^0 which can result in a slight modification of the traditional directional element theory. The directional element function will now be solely based on the magnitude of negative-sequence reactance or in other words, based on the direction of negative-sequence reactive power (numerator of eq.3.7). With this ECA setting, the necessity of mentioning I_2-active in inverter control to a non-positive value as specified in the recommendation point-3 can be avoided. This I_2-active still can be used for other control objectives like mitigating double-frequency oscillations, etc.

CHAPTER 5: CONCLUSIONS

This chapter presents the summary of work done, Conclusion, and future work.

5.1 Summary of Work Done

Inverter-based wind power plants use in power system is increasing, and also their challenges on protection systems. Protection systems developed based on traditional sources short circuit behavior, expect the same short circuit behavior from the IBRs. Challenges are observed from the real-time scenarios for negative-sequence directional element's application to the Type-IV WPP. This thesis work analyzed the performance of the negative-sequence directional element for a Type-IV WPP under various control methodologies such as CC, DSC-1, and DSC-2 (German grid code). To examine the negative-sequence directional element use for the Type-IV WPPs, this work first analyzed the directional element application for the traditional sources. Then, traditional source short circuit behavior compared with the Type-IV WPP short circuit behavior. German grid code implemented Type-IV WPP short circuit behavior observed to have similarities with a traditional source (weak source). Directional element results are analyzed for several fault cases for Type-IV WPP with three control schemes to identify suitable control schemes and to identify cases where the directional element is failing. From the results obtained, German grid code based control scheme found to be more suitable for negative-sequence directional element application. Even though the German grid code control model is more promising, it also has few shortcomings. To counter the shortcomings from the German grid code implemented Type-IVV WPP, recommendations are provided to have additional requirements from the inverter control system such as, negative-sequence active current

requirements, and minimum $|I_2|/|I_1|$ feature. Recommendations are also provided for the relay logic changes such as modifying a2 setting and ECA setting, to improve the directional element performance. Improved results are presented after implementing the modified relay logic from $|I_2|/|I_1|$ to $|I_2\text{-reactive}|/|I_1\text{-reactive}|$.

5.2 Conclusion

The performance of the negative-sequence directional element was analyzed for Type-IV WPP with controls CC, DSC-1 and DSC-2 (German grid code). The DSC-2 control model was observed to be the most promising. This control model converts the negative-sequence system from IBR to fault point into purely inductive, irrespective of the system resistance and inductance. This purely inductive behavior is in line with traditional source fault behavior, except for the fact that the IBR offers lower negative-sequence currents without active current component. Hence, the negative-sequence directional element based on traditional source fault behavior can be applied on IBRs with DSC-2 control that follows the German grid code reactive current requirements. By further addressing the negative-sequence active current requirements to the German grid code-based control system, and/or by modifying the directional element logic as proposed, the use, dependability, and security of the negative-sequence directional element for Type-IV WPP can be further improved.

5.3 Future Work

IBR offers many challenges for the protection functions. This research is focused on negative-sequence directional element. This section presents the work not covered in this thesis and requires studying further for IBRs.

- Extend the work to Type−III wind power plants.
- Various control schemes, which can be possible even after obeying the German grid code requirements, may be studied further (for example, mixing DSC-1 control objectives in DSC-2 controls).

- Extend the work to other protection functions like fault identification, fault location, distance protection, etc.
- Protection functions which operates within first 1 or 2 cycles like incremental quantities and traveling wave-based protection functions are to be studied further using detailed models.

REFERENCES

[1] M. Nagpal and C. Henville, "Impact of power-electronic sources on transmission line ground fault protection," *IEEE Transactions on Power Delivery*, vol. 33, no. 1, pp. 62–70, 2017.

[2] O. Ellabban, H. Abu-Rub, and F. Blaabjerg, "Renewable energy resources: Current status, future prospects and their enabling technology," *Renewable and Sustainable Energy Reviews*, vol. 39, pp. 748–764, 2014.

[3] E. Muljadi, N. Samaan, V. Gevorgian, J. Li, and S. Pasupulati, "Short circuit current contribution for different wind turbine generator types," in *IEEE PES General Meeting*, pp. 1–8, IEEE, 2010.

[4] J. Barsch, G. Bartok, G. Benmouya, O. Bolado, B. Boysen, S. Brahma, S. Brettschneider, Z. Bukhala, and J. Burnworth, "Fault current contributions from wind plants," *A Report to the T&D Committee, Electric Machinery Committee and Power System Relaying Committee of the IEEE PES*, 2012.

[5] M. Chaudhary, S. M. Brahma, and S. J. Ranade, "Short circuit analysis of type ii induction generator and wind farm," in *PES T&D 2012*, pp. 1–5, IEEE, 2012.

[6] A. Rajapakse, R. Majumder, S. G. R. Energy, and R. Nelson, "Modification of commercial fault calculation programs for wind turbine generators,"

[7] L. Hadjidemetriou, E. Kyriakides, and F. Blaabjerg, "A new hybrid pll for interconnecting renewable energy systems to the grid," *IEEE Transactions on industry applications*, vol. 49, no. 6, pp. 2709–2719, 2013.

[8] M. G. Taul, X. Wang, P. Davari, and F. Blaabjerg, "Robust fault ride-through of converter-based generation during severe faults with phase jumps," *IEEE Transactions on Industry Applications*, 2019.

[9] P. Rodríguez, J. Pou, J. Bergas, J. I. Candela, R. P. Burgos, and D. Boroyevich, "Decoupled double synchronous reference frame pll for power converters control," *IEEE Transactions on Power Electronics*, vol. 22, no. 2, pp. 584–592, 2007.

[10] V. Kaura and V. Blasko, "Operation of a phase locked loop system under distorted utility conditions," *IEEE Transactions on Industry applications*, vol. 33, no. 1, pp. 58–63, 1997.

[11] M. Karimi-Ghartemani, M. Iravani, and F. Katiraei, "Extraction of signals for harmonics, reactive current and network-unbalance compensation," *IEE Proceedings-Generation, Transmission and Distribution*, vol. 152, no. 1, pp. 137–143, 2005.

[12] J. K. Petter, "Methods, systems, and software for controlling a power converter during low (zero)-voltage ride-through conditions," June 14 2012. US Patent App. 13/275,362.

[13] R. Teodorescu, M. Liserre, and P. Rodriguez, *Grid converters for photovoltaic and wind power systems*, vol. 29. John Wiley & Sons, 2011.

[14] K. W. Jones, P. Pourbeik, G. Kobet, *et al.*, "Impact of inverter based generation on bulk power system dynamics and short-circuit performance," *Task Force on Short-Circuit and System Performance Impact of Inverter Based Generation, Tech. Rep. PESTR68*, 2018.

[15] B. Chen, A. Shrestha, F. A. Ituzaro, and N. Fischer, "Addressing protection challenges associated with type 3 and type 4 wind turbine generators," in *2015 68th Annual Conference for Protective Relay Engineers*, pp. 335–344, IEEE, 2015.

[16] C. Holt and M. J. Thompson, "Practical considerations when protecting mutually coupled lines," in *2016 69th Annual Conference for Protective Relay Engineers (CPRE)*, pp. 1–16, IEEE, 2016.

[17] N. Fisher, "Protection of inverter-based resources," *Article published in ESIG*, January 2020.

[18] E. O. Schweitzer III and J. J. Kumm, "Statistical comparison and evaluation of pilot protection schemes," in *Proc. of the 23rd Western Protective Relay Conference*, pp. 15–17, 1996.

[19] U. Karaagac, J. Mahseredjian, R. Gagnon, H. Gras, H. Saad, L. Cai, I. Kocar, A. Haddadi, E. Farantatos, S. Bu, *et al.*, "A generic emt-type model for wind parks with permanent magnet synchronous generator full size converter wind turbines," *IEEE Power and Energy Technology Systems Journal*, vol. 6, no. 3, pp. 131–141, 2019.

[20] J. Roberts and A. Guzman, "Directional element design and evaluation," in *proceedings of the 21st Annual Western Protective Relay Conference, Spokane, WA*, 1994.

[21] K. Zimmerman and D. Costello, "Fundamentals and improvements for directional relays," in *2010 63rd Annual Conference for Protective Relay Engineers*, pp. 1–12, IEEE, 2010.

[22] *SEL-421 Instruction Manual (Available: https://selinc.com)*.

[23] E. Camm, M. Behnke, O. Bolado, M. Bollen, M. Bradt, C. Brooks, W. Dilling, M. Edds, W. Hejdak, D. Houseman, *et al.*, "Characteristics of wind turbine generators for wind power plants," in *2009 IEEE Power & Energy Society General Meeting*, pp. 1–5, ieee, 2009.

[24] S.-H. Ko, S. R. Lee, H. Dehbonei, and C. V. Nayar, "Application of voltage-and current-controlled voltage source inverters for distributed generation systems," *IEEE Transactions on Energy Conversion*, vol. 21, no. 3, pp. 782–792, 2006.

[25] A. Abdalrahman, A. Zekry, and A. Alshazly, "Simulation and implementation of grid-connected inverters," *International Journal of Computer Applications*, vol. 60, no. 4, 2012.

[26] P. Rodriguez, A. Luna, R. S. Munoz-Aguilar, I. Etxeberria-Otadui, R. Teodorescu, and F. Blaabjerg, "A stationary reference frame grid synchronization system for three-phase grid-connected power converters under adverse grid conditions," *IEEE transactions on power electronics*, vol. 27, no. 1, pp. 99–112, 2012.

[27] P. C. Krause, O. Wasynczuk, S. D. Sudhoff, and S. Pekarek, *Analysis of electric machinery and drive systems*, vol. 2. Wiley Online Library, 2002.

[28] J.-P. Matsinen, "Standards and grid codes â the latest developments and trends,"

[29] "Guide to the IEEE 1547-2018 standard and its impacts on cooperatives," *Available from (https://www.nrel.gov/grid/ieee-standard-1547/cooperatives-impacts.html)*, March 2019.

[30] "NERC Standard PRC-024-2 Generator Frequency and Voltage Protective Relay Settings," *Available from (https://www.nerc.com/pa/Stand/Reliability Standards/PRC-024-2.pdf)*, 2016.

[31] "Technical connection rules for high-voltage (vde-ar-n 4120)," *Available in (https://www.vde.com/en/fnn/topics/technical-connection-rules/tar-for-high-voltage)*, October 2018.

[32] A. Guzman, J. Roberts, and D. Hou, "New ground directional elements operate reliably for changing system conditions," in *23rd Annual Western Protective Relay Conference*, 1996.

[33] Y. Levron, J. Belikov, and D. Baimel, "A tutorial on dynamics and control of power systems with distributed and renewable energy sources based on the dq0 transformation," *Applied Sciences*, vol. 8, no. 9, p. 1661, 2018.

[34] A. Haddadi, I. Kocar, T. Kauffmann, U. Karaagac, E. Farantatos, and J. Mahseredjian, "Field validation of generic wind park models using fault records," *Journal of Modern Power Systems and Clean Energy*, vol. 7, no. 4, pp. 826–836, 2019.

[35] U. Karaagac, J. Mahseredjian, H. Gras, H. Saad, J. Peralta, and L. Bellomo, "Simulation models for wind parks with variable speed wind turbines in emtp-rv," *Polytechnique Montréal*, 2017.